Nonsmooth SOR for L^1-fitting: Convergence study and discussion of related issues

R. Glowinski, Houston **T. Kärkkäinen**, Jyväskylä
T. Valkonen, Jyväskylä **A. Ivannikov**, Jyväskylä

June 12, 2008

Abstract

In this article, the denoising of smooth (H^1-regular) images is considered. To reach this objective, we introduce a simple and highly efficient over-relaxation technique for solving the convex, non-smooth optimization problems resulting from the denoising formulation. We describe the algorithm, discuss its convergence and present the results of numerical experiments, which validate the methods under consideration with respect to both efficiency and denoising capability. Several issues concerning the convergence of an Uzawa algorithm for the solution of the same problem are also discussed.

AMS Subject Classification: 68U10, 90C30
Key words: denoising, non-smooth objective function, convex analysis, over-relaxation

1 Introduction

In this article, we consider numerical methods for solving the following nonsmooth, strictly convex optimization problem

$$\min_{v\in V} \mathcal{J}(v), \quad \mathcal{J}(v) = \int_\Omega \left[|v-z| + \frac{\beta_1}{2}\left|\frac{\partial v}{\partial x_1}\right|^2 + \frac{\beta_2}{2}\left|\frac{\partial v}{\partial x_2}\right|^2 \right] d\boldsymbol{x}, \tag{1}$$

where Ω is a domain in $\mathbb{R}^2$ (a rectangle in many applications); $\beta_1, \beta_2 > 0$ denote regularization parameters; $d\boldsymbol{x} = dx_1 dx_2$; and V is a closed vector or affine subspace of $H^1(\Omega)$ (it can be $H^1(\Omega)$ itself).

As discussed and thoroughly tested in [11], the denoising approach based on formulation (1) is very efficient in cases, where the noise contained in the original image (observation) z is not due to a single normal distribution with fixed variance, but contains outliers and other degradations due to mixed and varying characteristics of the noise distribution (e.g. [8, 19, 18]). This case also includes the so-called "salt and pepper noise" [1].

To elucidate the practical usability of the considered formulation, let us give immediately an example illustrated in Figure 1. The example is related to slow-combustion (smouldering)

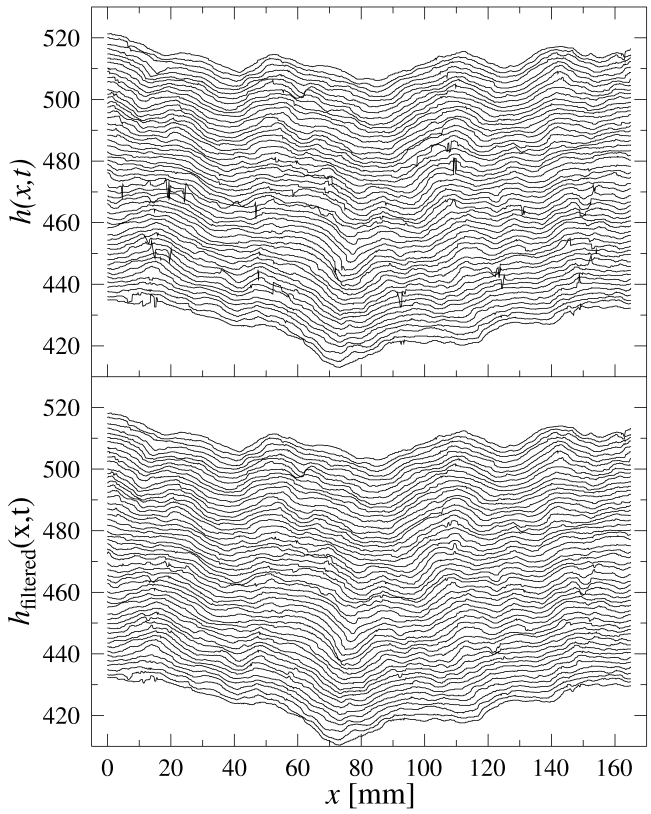

Figure 1: Front profiles of a lens-paper burn before ($h(x,t)$) and after ($h_{\text{filtered}}(x,t)$) filtering the data [16].

fronts propagating in burning sheets of paper [16]. The process can be modelled using the Kardar-Parisi-Zhang (KPZ) equation

$$\partial_t h = c + \nu\Delta h + \frac{\lambda}{2}(\nabla h)^2 + \eta, \tag{KPZ}$$

where $h \equiv h(x,t)$ is the height of the interface, c its zero-slope velocity, and η denotes the effective noise [10]. In order to characterize the burning material using the model parameters c, ν, and λ, the propagation of the emerging one-dimensional front was recorded with a CCD-camera system. Outliers in the resulting image were caused by, e.g., ash particles detached from the front. The denoising in this example turned out to be very successfull, because the unrealistic points (pixel values) showing nonphysical decrease of the height of the burning front were removed but the local variation remained, which allowed the estimation of the unknown model parameters with a sufficient accuracy using local fitting techniques [16]. The numerical results in this paper are also based on a few real recordings related to this application. Based on this real data, we present a comparison of the results based on (1) with those obtained with some classical methods for image processing ([9, 15]) to validate the approach here.

The basic difficulty concerning the image denoising problem with L^1-fitting is its nondif-

ferentiability in the classical sense, although the recent trend introducing even more severe nonsmoothness in optimization based image restoration is to consider formulations with nonsmooth BV/TV-type regularization. For an excellent description of various formulations and related algorithms, and a suggestion to determine an appropriate regularization parameter we refer to [1] and articles therein. Properties related to the use of L^1-norm for image denoising have been studied in e.g. [18].

From an algorithmic point of view, we investigated and developed in [11] an *active-set method* (ASM) for solving the discrete problem resulting from finite element discretization of (1). Being able to solve problems with hundreds of thousands of unknowns, we feel that this is a successfull method for a nonsmooth optimization problem. However, the efficiency of ASM relies on the corresponding efficiency of a linear system solver for a Poisson problem on a sequence of varying and highly irregular geometries. Both the geometrical reasons (e.g. unstructured grid to capture corner singularities for complicated domains) and the needed amount of memory (CG method with multigrid preconditioner, see [13, 12]) are both good reasons to consider alternative solution methods for (1). The successive over-relaxation methods discussed in this article for solving (1) are clearly related to the ones discussed in [2, 3] and [5] for the solution of problems from *nonsmooth mechanics*. To the best of our knowledge they have never been applied to image processing with L^1-fitting.

The content of the article is as follows: In Section 2, assuming that $V = H_0^1(\Omega)$, we provide several characterizations of the unique solution of problem (1) and discuss various consequences, including some which have computational implications. In Section 3, we discuss the finite element approximation of problem (1). In Section 4, we discuss the iterative solution of problem (1) and of its finite element analogues with a particular emphasis on a SOR type algorithm; for this last algorithm we will introduce a strategy for varying the relaxation parameter at each time step and will prove that it guarantees the convergence. In Section 5, we will discuss the implications of taking $V = H^1(\Omega)$ in (1), a reasonable assumption indeed, from a practical point of view; we will show that we still have existence of solutions, but that uniqueness is a problematic issue, that we will discuss with some details in both the continuous and discrete cases. Finally, in Section 6 we present and discuss the results of numerical experiments.

2 Existence, uniqueness and characterizations of the solution to problem (1)

Suppose for simplicity that $V = H_0^1(\Omega)$ (the more complicated case $V = H^1(\Omega)$ will be considered in Section 5); suppose also that $z \in L^2(\Omega)$ (which covers all practical applications). Since Ω is bounded, the mapping

$$v \mapsto \sqrt{\beta_1 \left\| \frac{\partial v}{\partial x_1} \right\|^2_{L^2(\Omega)} + \beta_2 \left\| \frac{\partial v}{\partial x_2} \right\|^2_{L^2(\Omega)}} : H^1(\Omega) \to \mathbb{R}$$

defines over $H_0^1(\Omega)$ a Hilbertian norm, *equivalent* to the one induced by $H^1(\Omega)$. The functional $v \mapsto \|v - z\|_{L^1(\Omega)}$ is *convex* and *continuous* over $L^2(\Omega)$, and therefore over $H_0^1(\Omega)$.

From these properties, problem (1) (a classical problem from *Calculus of Variations*) has a *unique solution* u characterized by (cf., e.g., [3, Lemma I.4.1], [5]):

$$\begin{aligned} &u \in H_0^1(\Omega), \\ &\int_\Omega \left[\beta_1 \frac{\partial}{\partial x_1}(v-u)\frac{\partial u}{\partial x_1} + \beta_2 \frac{\partial}{\partial x_2}(v-u)\frac{\partial u}{\partial x_2}\right] dx + j(v) - j(u) \geq 0,\ \forall v \in H_0^1(\Omega), \end{aligned} \tag{2}$$

where

$$j(v) = \int_\Omega |v-z| dx,\ \forall v \in L^1(\Omega)\,(\supset H_0^1(\Omega)).$$

Variational problems such as (2) are known as *variational inequalities* (of the second kind, by some authors); constructive methods for the solution of a large selection of variational inequalities (mostly from Mechanics and Physics) can be found in, e.g., [3], [5].

Remark 2.1. *In the non-differentiable context associated with the functional $j(\cdot)$ relation* (2) *plays the role of the Euler-Lagrange equations associated to the differentiable problems from Calculus of Variations.*

Remark 2.2. *An equivalent formulation of* (2) *is provided by the following (multi-valued) equation:*

$$\begin{aligned} &u \in H_0^1(\Omega), \\ &-\beta_1 \frac{\partial^2 u}{\partial x_1^2} - \beta_2 \frac{\partial^2 u}{\partial x_2^2} + \partial j(u) \ni 0, \end{aligned} \tag{3}$$

where $\partial j(u)$ is the sub-gradient *of $j(\cdot)$ at u.*

Another equivalent *characterization of the solution is provided by*

$$\begin{aligned} &u \in H_0^1(\Omega), \lambda \in \Lambda = \{\mu \in L^2(\Omega) \mid |\mu(x)| \leq 1 \ a.e.\ in\ \Omega\}, \\ &-\beta_1 \frac{\partial^2 u}{\partial x_1^2} - \beta_2 \frac{\partial^2 u}{\partial x_2^2} + \lambda = 0 \ in\ \Omega, \\ &\lambda(u-z) = |u-z|, \end{aligned} \tag{4}$$

which, in some sense, makes (3) *more precise by identifying the unique element of $\partial j(u)$ (namely λ) for which the inclusion in* (3) *reduces to an equation in $L^\infty(\Omega)$. Incidentally, if the boundary Γ of Ω is* smooth *and/or Ω is convex, the property $\lambda \in \Lambda(\subset L^\infty(\Omega))$ implies $u \in W^{2,p}(\Omega)$ for all $p \in [1, +\infty)$, which implies in turn (from one of the* Sobolev imbedding theorems*; see, e.g., [17]) that $u \in C^{1,\alpha}(\bar{\Omega})$ for all $\alpha \in [0,1)$, i.e., it has "almost" the $C^2(\bar{\Omega})$-regularity.*

Remark 2.3. *It can be shown (see, e.g., [3], [5]) that the system* (4) *characterizes the pair $\{u, \lambda\}$ as a saddle-point over $H_0^1(\Omega) \times \Lambda$ of the Lagrangian functional L defined by:*

$$L(v,\mu) = \frac{1}{2}\int_\Omega (\beta_1 |\partial v/\partial x_1|^2 + \beta_2 |\partial v/\partial x_2|^2) dx + \int_\Omega \mu(v-z) dx.$$

Following [3], [5] (see, also [4, Chapter 4]) the above observation suggests to solve problem (1)*, via the equivalent system* (4)*, using the* Uzawa type algorithm *of the form:*

$$\lambda^0 \text{ is given in } \Lambda \quad (\lambda^0 = 0, \text{ for example}). \tag{5}$$

For $n \geq 0$, λ^n being known, compute u^n and λ^{n+1} as follows: solve

$$u^n \in H_0^1(\Omega), \quad -\beta_1 \frac{\partial^2 u^n}{\partial x_1^2} - \beta_2 \frac{\partial^2 u^n}{\partial x_2^2} + \lambda^n = 0 \text{ in } \Omega, \tag{6}$$

$$\lambda^{n+1} = P_\Lambda[(\lambda^n + \rho(u^n - z)], \tag{7}$$

where P_Λ, the orthogonal projection operator *from $L^2(\Omega)$ onto Λ, is defined by*

$$P_\Lambda(\mu)(x) = \inf[1, \sup[-1, \mu(x)]], \text{ a.e. in } \Omega, \forall \mu \in L^2(\Omega).$$

We observe that, for obvious reasons, u^n has the same regularity properties as u, namely

$$u^n \in H_0^1(\Omega) \cap W^{2,p}(\Omega), \forall p \in [1, +\infty)$$

Theorem 2.1. *Suppose that*

$$0 < \rho < 2 \min(\beta_1, \beta_2)\kappa_0, \tag{8}$$

where, in (8)*, κ_0 is the* smallest eigenvalue of the operator $-\Delta$ *in $H_0^1(\Omega)$. Then, for all $\lambda_0 \in \Lambda$, $s < 2$, and $p \in [1, +\infty)$, we have*

$$\lim_{n \to +\infty} u^n = u \text{ in } W^{s,p}(\Omega), \tag{9}$$

where u is the solution of problem (1)*.*

Proof. Denote $u^n - u$ and $\lambda^n - \lambda$ by $\bar{u}^n$ and $\bar{\lambda}^n$, respectively. From (6) and (7) we then have by subtraction and since the operator P_Λ is a contraction of $L^2(\Omega)$:

$$\bar{u}^n \in H_0^1(\Omega), \quad -\beta_1 \frac{\partial^2 \bar{u}^n}{\partial x_1^2} - \beta_2 \frac{\partial^2 \bar{u}^n}{\partial x_2^2} + \bar{\lambda}^n = 0 \text{ in } \Omega, \tag{10}$$

and

$$\left\| \bar{\lambda}^{n+1} \right\|_{0,\Omega} \leq \left\| \bar{\lambda}^n + \rho \bar{u}^n \right\|_{0,\Omega}, \tag{11}$$

where $\| \cdot \|_{0,\Omega} = \| \cdot \|_{L^2(\Omega)}$. Relations (10) and (11) imply in turn that

$$\int_\Omega \left[\beta_1 \frac{\partial \bar{u}^n}{\partial x_1} \frac{\partial v}{\partial x_1} + \beta_2 \frac{\partial \bar{u}^n}{\partial x_2} \frac{\partial v}{\partial x_2} \right] dx + \int_\Omega \bar{\lambda}^n v dx = 0, \forall v \in H_0^1(\Omega), \tag{12}$$

and

$$\|\bar{\lambda}^n\|_{0,\Omega}^2 - \|\bar{\lambda}^{n+1}\|_{0,\Omega}^2 \geq -2\rho \int_\Omega \bar{\lambda}^n \bar{u}^n dx - \rho^2 \|\bar{u}^n\|_{0,\Omega}^2. \tag{13}$$

Taking $v = \bar{u}^n$ in (12) and combining with (13) and the well-known inequality

$$\|\nabla v\|_{0,\Omega}^2 \geq \kappa_0 \|v\|_{0,\Omega}^2, \forall v \in H_0^1(\Omega),$$

(where κ_0 is the smallest eigenvalue of $-\Delta$ operating in $H_0^1(\Omega)$) yields

$$\|\bar{\lambda}^n\|_{0,\Omega}^2 - \|\bar{\lambda}^{n+1}\|_{0,\Omega}^2 \geq \rho[2\min(\beta_1,\beta_2) - \kappa_0^{-1}\rho]\|\nabla\bar{u}^n\|_{0,\Omega}^2. \tag{14}$$

Suppose that the condition (8) holds; then the sequence $\{\|\bar{\lambda}^n\|_{0,\Omega}^2\}_{n\geq 0}$ is decreasing; since it is bounded from below by 0, it converges to some (non-negative) limit, implying from (14) that

$$\lim_{n\to+\infty} \nabla\bar{u}^n = 0 \text{ in } (L^2(\Omega))^2,$$

i.e.

$$\lim_{n\to+\infty} u^n = u \text{ in } H_0^1(\Omega). \tag{15}$$

Combining (15) and (10), we can show (we skip the details) that

$$\lambda^n \to \lambda \text{ in } H^{-1}(\Omega) \cap (L^\infty(\Omega) \text{ weak-}^*),$$

which implies in turn that

$$u^n \to u \text{ weakly in } W^{2,p}(\Omega), \forall p \in [1,+\infty). \tag{16}$$

The injection of $W^{2,p}(\Omega)$ into $W^{s,p}(\Omega)$ being *compact* if $s < 2$, relation (16) implies the convergence result (9), and also

$$u^n \to u \text{ in } C^{1,\alpha}(\bar{\Omega}),\ \forall \alpha \in [0,1).$$

□

This concludes Remark 2.3 (algorithm (5)-(7) *deserves further comments, some of them will be given in following remarks).*

Remark 2.4. *The equivalent system* (4) *has proved already quite useful by: (i) bringing information on the regularity of the solution u of problem* (1)*; (ii) leading us to an iterative method quite easy to implement in order to compute the solution. Actually, system* (4) *can tell us more. Indeed, suppose that*

$$z \in W^{2,\infty}(\Omega) \cap H_0^1(\Omega). \tag{17}$$

(A very strong assumption, implying that there is no need for the problem (1) *based L^1-smoothing, since, from* (4)*, it does not bring more than the $W^{2,\infty}(\Omega)$-regularity, precisely.) Multiplying by $u - z$ both sides of the elliptic equation in* (4)*, we obtain, after integration by parts, that*

$$\int_\Omega \left[\beta_1 \frac{\partial u}{\partial x_1}\frac{\partial}{\partial x_1}(u-z) + \beta_2 \frac{\partial u}{\partial x_2}\frac{\partial}{\partial x_2}(u-z)\right] dx + \|u-z\|_{L^1(\Omega)} = 0. \tag{18}$$

Denote $u - z$ by w. It follows then from (18) *that*

$$\int_\Omega \left[\beta_1 \left|\frac{\partial w}{\partial x_1}\right|^2 + \beta_2 \left|\frac{\partial w}{\partial x_2}\right|^2\right] dx + \int_\Omega \left[\beta_1 \frac{\partial w}{\partial x_1}\frac{\partial z}{\partial x_1} + \beta_2 \frac{\partial w}{\partial x_2}\frac{\partial z}{\partial x_2}\right] dx + \|w\|_{L^1(\Omega)} = 0. \tag{19}$$

Integrating by parts in the second integral in the left-hand side of (19) *we obtain:*

$$\int_\Omega \left[\beta_1 \left|\frac{\partial w}{\partial x_1}\right|^2 + \beta_2 \left|\frac{\partial w}{\partial x_2}\right|^2\right] dx - \int_\Omega \left[\beta_1 \frac{\partial^2 z}{\partial x_1^2} + \beta_2 \frac{\partial^2 z}{\partial x_2^2}\right] w dx + \|w\|_{L^1(\Omega)} = 0. \tag{20}$$

Let us denote by $\boldsymbol{\beta}$ *the vector* $\{\beta_1, \beta_2\}$ *and by* $|\boldsymbol{\beta}| = \sqrt{\beta_1^2 + \beta_2^2}$ *the Euclidian norm of this vector. It follows from* (20) *and the Schwarz inequality in* $\mathbb{R}^2$ *and from the Young inequality that*

$$\int_\Omega \left[\beta_1 \left|\frac{\partial w}{\partial x_1}\right|^2 + \beta_2 \left|\frac{\partial w}{\partial x_2}\right|^2\right] dx + \|w\|_{L^1(\Omega)} \left(1 - |\boldsymbol{\beta}| \sqrt{\left\|\frac{\partial^2 z}{\partial x_1^2}\right\|^2_{L^\infty(\Omega)} + \left\|\frac{\partial^2 z}{\partial x_2^2}\right\|^2_{L^\infty(\Omega)}}\right) \leq 0. \tag{21}$$

It then follows from (21) *that*

$$u = z \text{ if } |\boldsymbol{\beta}| \leq 1/\sqrt{\left\|\frac{\partial^2 z}{\partial x_1^2}\right\|^2_{L^\infty(\Omega)} + \left\|\frac{\partial^2 z}{\partial x_2^2}\right\|^2_{L^\infty(\Omega)}}. \tag{22}$$

For less smooth functions z*, the relation* $u = z$ *will take place, if and only if* $\boldsymbol{\beta} = 0$*.*

Remark 2.5. *The numerical experiments reported in [11] show that the number of iterations (*nit*) required for the convergence of the discrete analogue of the Uzawa algorithm* (5)-(7) *increases with* $1/|\boldsymbol{\beta}|$ *(*z *staying the same). Actually, for "small" values of* $|\boldsymbol{\beta}|$, nit *becomes prohibitively large, making the active set method (ASM), thoroughly discussed in [11], a very attractive alternative. As we will see in Section 4, one of the main features of the over-relaxation method discussed here is that its performance improves as* $\boldsymbol{\beta}$ *gets smaller, a behavior it shares with the ASM algorithms discussed in [11]. In order to comprehend why the performances of the Uzawa algorithm* (5)-(7) *deteriorate when* $|\boldsymbol{\beta}|$ *gets smaller (*z *staying the same) we are going to return to system* (4)*, assuming that* $\beta_1 = \beta_2 = \beta$*, for simplicity. First we observe that* (4) *implies*

$$\lambda \in \Lambda,\ u = -\beta^{-1}(-\Delta)^{-1}\lambda \tag{23}$$

and

$$\int_\Omega (z - u)(\mu - \lambda) dx \geq 0,\ \forall \mu \in \Lambda. \tag{24}$$

In (23)*,* $(-\Delta)^{-1}$ *denotes the inverse of* $-\Delta$ *for the homogeneous Dirichlet boundary conditions; from now on we will denote by* G *(for Green) the above operator* $(-\Delta)^{-1}$*. Operator* G *is self-adjoint, compact and positive definite over* $L^2(\Omega)$*; if* Γ *is smooth enough and/or* Ω *is convex, then* G *is an isomorphism from* $L^2(\Omega)$ *onto* $H_0^1(\Omega) \cap H^2(\Omega)$*. Combining* (23) *and* (24) *yields*

$$\lambda \in \Lambda, \quad \int_\Omega (\beta^{-1} G\lambda + z)(\mu - \lambda) dx \geq 0, \forall \mu \in \Lambda. \tag{25}$$

The elliptic variational inequality (25) *is one of the many dual problems of* (1)*. Actually,* (25) *characterizes* λ *as the solution of the following minimization problem:*

$$\lambda \in \Lambda, \quad \mathcal{J}^*(\lambda) \leq \mathcal{J}^*(\mu),\ \forall \mu \in \Lambda \tag{26}$$

with

$$\mathcal{J}^*(\mu) = \frac{1}{2}\beta^{-1}\int_\Omega (G\mu)\mu dx + \int_\Omega z\mu dx,\ \forall \mu \in L^2(\Omega). \tag{27}$$

Problem (25), (26) *is well-posed from the boundedness of* Λ *and from the continuity and strict convexity of* $\mathcal{J}^*$ *over* $L^2(\Omega)$. *Since the differential* $D\mathcal{J}^*(\mu)$ *of* $\mathcal{J}^*$ *at* μ *verifies*

$$D\mathcal{J}^*(\mu) = \beta^{-1}G\mu + z,\ \forall \mu \in L^2(\Omega), \tag{28}$$

it follows then from (24)-(28) *that the Uzawa algorithm* (5)-(7) *can be rewritten as:*

$$\lambda^0 \text{ is given in } \Lambda. \tag{29}$$

For $n \geq 0$, *we obtain* λ^{n+1} *from* λ^n *via*

$$\lambda^{n+1} = P_\Lambda[\lambda^n - \rho(\beta^{-1}G\lambda^n + z)], \tag{30}$$

i.e., algorithm (5)-(7) *is a gradient method with projection. In order to study the dependence in* β *of the convergence of algorithm* (5)-(7), *we introduce* $\lambda_\beta = \beta^{-1}\lambda$, $\Lambda_\beta = \{\mu \in L^2(\Omega) \mid |\mu(x)| \leq \beta^{-1} \text{ a.e. in } \Omega\}$, *and, without loss of generality, replace* ρ *by* $\beta\rho$ *in* (7) *and* (30). *With obvious notation, algorithm* (5)-(7), (28)-(30) *can be rewritten as*

$$\lambda_\beta^0 \text{ is given in } \Lambda; \tag{31}$$

for $n \geq 0$, *we obtain* λ_β^{n+1} *from* λ_β^n *via*

$$\lambda_\beta^{n+1} = P_{\Lambda_\beta}[\lambda_\beta^n - \rho(\beta^{-1}G\lambda_\beta^n + z)]. \tag{32}$$

Concerning the convergence of algorithm (31), (32), $\forall \beta > 0$, *we have convergence of* $\{\lambda_\beta^n\}_{n\geq 0}$ *if the condition* $0 < \rho < 2\kappa_0$ *holds (where, as in* (8), κ_0 *is the smallest eigenvalue of* $-\Delta$ *in* $H_0^1(\Omega)$*). Since operator* G *lacks the* $L_2(\Omega)$*-ellipticity property (i.e., there is no* c (>0) *such that* $\int_\Omega (G\mu)\mu dx \geq c\,\|\mu\|^2_{L^2(\Omega)}$, $\forall \mu \in L^2(\Omega)$, *we can not expect the convergence to behave uniformly with respect to* β*; in that case, the factor dominating the convergence is the "size" of* Λ_β, *which increases with* β^{-1}, *making the target* λ_β *more costly to reach as* β *decreases (actually, unless* $z \in H^2(\Omega) \cap H_0^1(\Omega)$, *we can prove that* $\lim_{\beta\to 0_+} \|\lambda_\beta\|_{L^2(\Omega)} = +\infty$*).*

Remark 2.6. *Although this issue is of little interest with respect to* L^1*-fitting, we can wonder about the behavior of the solution of problem* (1) *when* $|\boldsymbol{\beta}| \to +\infty$. *In that direction, we can show that if* u *is the solution to problem* (1), *with* $V = H_0^1(\Omega)$, *then*

$$\lim_{\min\{\beta_1,\beta_2\}\to+\infty} u = 0 \text{ in } H_0^1(\Omega) \cap W^{2,p}(\Omega), \forall p \in [1, +\infty).$$

3 Finite element approximation of problem (1)

We suppose that Ω is a polygonal domain of $\mathbb{R}^2$. Next, we introduce a *triangulation* $\mathcal{T}_h$ of Ω whose vertices coincide with the original observation points, i.e., the pixel coordinates

defining the image to be denoised. We approximate then $H_0^1(\Omega)$ by the finite element space V_{0h} defined as follows:

$$V_{0h} = \{v \mid v \in C^0(\bar{\Omega}), v|_T \in P_1, \forall T \in \mathcal{T}_h, v = 0 \text{ on } \Gamma\}, \tag{33}$$

where P_1 is the space of polynomials in two variables of degree ≤ 1. Let Σ_{0h} be the set of the vertices of $\mathcal{T}_h$ which do not belong to Γ. We suppose that $\Sigma_{0h} = \{P_i\}_{i=1}^{N_{0h}}$, where $N_{0h} = \text{Card}(\Sigma_{0h})$. To Σ_{0h}, we associate the following vector basis of V_{0h}:

$$\mathcal{B}_{0h} = \{w_i\}_{i=1}^{N_{0h}}, \tag{34}$$

where the w_is are uniquely defined by

$$\begin{array}{l} w_i \in V_{0h}, \forall i = 1, \ldots, N_{0h}, \\ w_i(P_i) = 1, \forall i = 1, \ldots, N_{0h}; w_i(Q) = 0, \forall Q \text{ vertex of } \mathcal{T}_h, Q \neq P_i. \end{array} \tag{35}$$

We then have

$$v = \sum_{i=1}^{N_{0h}} v(P_i) w_i, \forall v \in V_{0h}. \tag{36}$$

Finally, we denote by α_i the area of the polygonal domain which is the union of the triangles of $\mathcal{T}_h$ which have P_i as a common vertex.

Using the above space V_{0h}, we approximate problem (1) associated to $V = H_0^1(\Omega)$ by

$$\text{Find } u_h \in V_{0h} \text{ such that } J_h(u_h) \leq J_h(v), \forall v \in V_{0h}, \tag{37}$$

where

$$J_h(v) = \frac{1}{2} \int_\Omega \left[\beta_1 \left| \frac{\partial v}{\partial x_1} \right|^2 + \beta_2 \left| \frac{\partial v}{\partial x_2} \right|^2 \right] dx + \frac{1}{3} \sum_{i=1}^{N_{0h}} \alpha_i \left| v(P_i) - z_i \right|. \tag{38}$$

Using, for example, the methods discussed in [3, Section I.6] and [5] we can prove that the approximate problem (37) has a unique solution characterized by

$$\begin{array}{l} u_h \in V_{0h}, \\ \displaystyle\int_\Omega \left[\beta_1 \frac{\partial u_h}{\partial x_1} \frac{\partial (v - u_h)}{\partial x_1} + \beta_2 \frac{\partial u_h}{\partial x_2} \frac{\partial (v - u_h)}{\partial x_2} \right] dx \\ \quad + \displaystyle\frac{1}{3} \left[\sum_{i=1}^{N_{0h}} \alpha_i \left| v(P_i) - z_i \right| - \sum_{i=1}^{N_{0h}} \alpha_i \left| u_h(P_i) - z_i \right| \right] \geq 0, \forall v \in V_{0h}. \end{array} \tag{39}$$

From the above two references we can also prove that if: (i) For example, $z_i = z(P_i)$ with $z \in C^0(\bar{\Omega})$; (ii) h is the length of the largest edge(s) of $\mathcal{T}_h$; (iii) $\forall h$, the angles of $\mathcal{T}_h$ are bounded from below by $\theta_0 > 0$, then

$$\lim_{h \to 0} u_h = u \text{ in } H_0^1(\Omega), \tag{40}$$

u being the solution of problem (1).

Remark 3.1. *If we fix h, then:* $\lim_{\beta\to 0} u_h = \sum_{i=1}^{N_{0h}} z_i w_i$.

Remark 3.2. *In* (39)*, assume that* $v = \sum_{i=1}^{N_{0h}} v_i w_i$ *and* $u_h = \sum_{i=1}^{N_{0h}} u_i w_i$*, and denote* $\{v_i\}_{i=1}^{N_{0h}}$ *and* $\{u_i\}_{i=1}^{N_{0h}}$ *by* $\boldsymbol{v}$ *and* $\boldsymbol{u}$*, respectively. The approximate problem* (39) *takes then the following (equivalent) formula:*

$$\begin{aligned} &\boldsymbol{u} \in \mathbb{R}^{N_{0h}}, \\ &(\beta_1 \boldsymbol{A}_1 + \beta_2 \boldsymbol{A}_2)\boldsymbol{u} \cdot (\boldsymbol{v} - \boldsymbol{u}) + j_h(\boldsymbol{v}) - j_h(\boldsymbol{u}) \geq 0,\ \forall \boldsymbol{v} \in \mathbb{R}^{N_{0h}}, \end{aligned} \tag{41}$$

where the matrices $\boldsymbol{A}_1$ *and* $\boldsymbol{A}_2$ *are both symmetric and positive definite;* $\boldsymbol{x} \cdot \boldsymbol{y} = \sum_{i=1}^{N_{0h}} x_i y_i$ $\forall x = \{x_i\}_{i=1}^{N_{0h}}$ *and* $y = y_{i\,i=1}^{N_{0h}} \in R^{N_{0h}}$*; and we have*

$$j_h(\boldsymbol{v}) = \sum_{i=1}^{N_{0h}} \alpha_i \left| v_i - z_i \right|,\ \forall \boldsymbol{v} = \{v_i\}_{i=1}^{N_{0h}} \in \mathbb{R}^{N_{0h}}.$$

System (41) *characterizes* u *as the unique solution of the following minimization problem (equivalent to* (37)*):*

$$\min_{\boldsymbol{v}} [\frac{1}{2}(\beta_1 \boldsymbol{A}_1 + \beta_2 \boldsymbol{A}_2)\boldsymbol{v} \cdot \boldsymbol{v} + j_h(\boldsymbol{v})],\ \textit{with}\ \boldsymbol{v} \in \mathbb{R}^{N_{0h}}. \tag{42}$$

Remark 3.3. *One can show (see, e.g., [11, Lemma 3.1]) that the solution* $\boldsymbol{u}$ *of problem* (41), (42) *is characterized by the existence of* $\boldsymbol{\lambda} = \{\lambda_i\}_{i=1}^{N_{0h}}$ *such that*

$$\begin{aligned} &(\beta_1 \boldsymbol{A}_1 + \beta_2 \boldsymbol{A}_2)\boldsymbol{u} \cdot \boldsymbol{v} + \sum_{i=1}^{N_{0h}} \alpha_i \lambda_i v_i = 0,\ \forall \boldsymbol{v} = \{v_i\}_{i=1}^{N_{0h}} \in \mathbb{R}^{N_{0h}}, \\ &|\lambda_i| \leq 1, \lambda_i(u_i - z_i) = |u_i - z_i|,\ \forall i = 1, \ldots N_{0h}. \end{aligned} \tag{43}$$

The system (43) *is clearly a* discrete analogue *of* (4)*. From* (43)*, we can derive an Uzawa algorithm for the solution of problem* (41), (42)*; such an algorithm has been investigated in [11]. An important consequence of* (43) *is that, in the discrete case, there is always a positive number* $\beta_{\min}$*, depending upon* $\boldsymbol{z} = \{z_i\}_{i=1}^{N_{0h}}$*, such that*

$$\boldsymbol{u} = \boldsymbol{z}\ \textit{if}\ |\boldsymbol{\beta}| \leq \beta_{\min},\ \textit{with}\ \beta_{\min} \geq A_{\min} / \sqrt{\|\boldsymbol{A}_1 z\|_\infty^2 + \|\boldsymbol{A}_2 z\|_\infty^2}, \tag{44}$$

with $A_{\min} = \min_i \alpha_i$*,* $i = 1, \ldots, N_{0h}$*, and* $\|\boldsymbol{y}\|_\infty = \max_i |y_i|$*,* $i = 1, \ldots, N_{0h}$*,* $\forall \boldsymbol{y} = \{y_i\}_{i=1}^{N_{0h}} \in \mathbb{R}^{N_{0h}}$*. Relation* (44) *(whose (easy) proof is left to the reader) is a discrete analogue of* (22)*. The lower bound of* $\beta_{\min}$ *in* (44) *depends on the smoothness of* z *(assuming that* $z_i = z(P_i)$*,* $\forall i = 1, \ldots, N_{0h}$*); it ranges, typically, from* $O(h^4)$*, if* z *is piecewise continuous, to* $O(1)$*, if* $z \in W^{2,\infty}(\Omega)$.

4 A point-wise over-relaxation method for the solution of the approximate problem

4.1 Generalities

In ref. [11], we discussed the iterative solution of problem (37), (39) by an active set method and by a discrete variant of the Uzawa algorithm (5)-(7). The results of the numerical experiments presented in [11] show clearly the superiority of the active set approach, particularly as

$\boldsymbol{\beta}$ gets smaller. Our goal here is to discuss a third method, of the point-wise over-relaxation type; see also [21]. After describing the algorithm (in Section 4.2), we will discuss its convergence (in Section 4.3). The *automatic adjustment of the relaxation parameter(s)* will also be addressed.

4.2 Description of the over-relaxation algorithm

The finite dimensional problem (41), (42) is a particular case of

$$\boldsymbol{u} \in \mathbb{R}^N, \quad J(\boldsymbol{u}) \leq J(\boldsymbol{v}), \forall \boldsymbol{v} \in R^N, \tag{45}$$

where $J(\boldsymbol{v}) = J_0(\boldsymbol{v}) + J_1(\boldsymbol{v})$, with

$$J_0(\boldsymbol{v}) = \frac{1}{2}\boldsymbol{A}\boldsymbol{v} \cdot \boldsymbol{v} - \boldsymbol{b} \cdot \boldsymbol{v}, \; \forall \boldsymbol{v} \in \mathbb{R}^N, \tag{46}$$

and

$$J_1(\boldsymbol{v}) = \sum_{i=1}^{N} \alpha_i \left| v_i - z_i \right|, \; \forall \boldsymbol{v} = \{v_i\}_{i=1}^N \in \mathbb{R}^N. \tag{47}$$

We suppose, in (46), (47), that $\boldsymbol{A}$ is an $N \times N$ matrix, symmetric and positive definite, that $\boldsymbol{b} = \{b_i\}_{i=1}^N \in \mathbb{R}^N$, and that $\alpha_i > 0$, $\forall i = 1, \ldots, N$. The minimization problem (45) has a *unique solution* characterized by

$$\boldsymbol{u} \in \mathbb{R}^N, \quad (\boldsymbol{A}\boldsymbol{u} - \boldsymbol{b}) \cdot (\boldsymbol{v} - \boldsymbol{u}) + J_1(\boldsymbol{v}) - J_1(\boldsymbol{u}) \geq 0, \; \forall \boldsymbol{v} \in \mathbb{R}^N. \tag{48}$$

Remark 4.1. *Compared with problem* (41), (42)*, we have included in* (45) *the linear functional* $\boldsymbol{v} \mapsto \boldsymbol{b} \cdot \boldsymbol{v}$*; this allows us to cover the situations where one wishes to make the change of variables* $\boldsymbol{v} \leftarrow \boldsymbol{v} - \boldsymbol{z}$ *and/or solve* (1) *when* $V = H_g^1(\Omega) = \{v \in H^1(\Omega) \mid v = g \text{ on } \Gamma\}$ *with* g *smooth enough* ($g \in C^0(\Gamma) \cap H^{1/2}(\Gamma)$*, typically).*

Following, e.g., [2, 3, 5], we advocate the following *relaxation algorithm*:

$$\boldsymbol{u}^0 = \{u_1^0, \ldots, u_N^0\} \text{ is given in } \mathbb{R}^n; \tag{49}$$

for $n \geq 0$, $\boldsymbol{u}^n = \{u_1^n, \ldots, u_N^n\}$ *being known we compute* $\boldsymbol{u}^{n+1} = \{u_1^{n+1}, \ldots, u_N^{n+1}\}$ as *follows*:

For $i = 1, \ldots, N$, solve the following one-dimensional minimization problem

$$\begin{aligned} &u_i^{n+1/2} \in \mathbb{R}, \\ &J(u_1^{n+1}, \ldots, u_{i-1}^{n+1}, u_i^{n+1/2}, u_{i+1}^n, \ldots, u_N^n) \leq J(u_1^{n+1}, \ldots, u_{i-1}^{n+1}, v, u_{i+1}^n, \ldots, u_N^n), \forall v_i \in \mathbb{R}, \end{aligned} \tag{50}$$

and compute

$$u_i^{n+1} = u_i^n + \omega_i^n (u_i^{n+1/2} - u_i^n) \quad (\text{with } \omega_i^n \in [1, 2)). \tag{51}$$

A strategy for the choice of ω_i^n, leading to the convergence of the relaxation algorithm, will be provided below. Concerning the solvability of problem (50), it follows from, e.g, [2, 3, 5], that problem (50) has a *unique solution* characterized by:

$$\begin{aligned} &u_i^{n+1/2} \in \mathbb{R}, \\ &\frac{\partial J_0}{\partial u_i}(u_1^{n+1}, \ldots, u_{i-1}^{n+1}, u_i^{n+1/2}, u_{i+1}^n, \ldots, u_N^n)(v_i - u_i^{n+1/2}) \\ &\quad + \alpha_i (|v_i - z_i| - \left| u_i^{n+1/2} - z_i \right|) \geq 0, \; \forall v_i \in \mathbb{R}. \end{aligned} \tag{52}$$

A more explicit form of (52) being (with obvious notation):

$$\begin{aligned} & u_i^{n+1/2} \in \mathbb{R}, \\ & (\sum_{j=1}^{i-1} a_{ij} u_j^{n+1} + a_{ii} u_i^{n+1/2} + \sum_{j=i+1}^{N} a_{ij} u_j^n - b_i)(v_i - u_i^{n+1/2}) \\ & \quad + \alpha_i (|v_i - z_i| - \left| u_i^{n+1/2} - z_i \right|) \geq 0, \, \forall v_i \in \mathbb{R}, \end{aligned} \tag{52'}$$

Actually, from (52'), we can easily show that

$$u_i^{n+1/2} = \min \left(\frac{b_i^{n+1/2} + \alpha_i}{a_{ii}}, \max(z_i, \frac{b_i^{n+1/2} - \alpha_i}{a_{ii}}) \right), \tag{53}$$

with

$$b_i^{n+1/2} = b_i - \sum_{j=1}^{i-1} a_{ij} u_j^{n+1} - \sum_{j=i+1}^{N} a_{ij} u_j^n. \tag{54}$$

From the practical point of view, (53) and (54) are the two most important relations of this article, since they allow explicit determinination of $u_i^{n+1/2}$. It follows from [2, 3, 5] that if one takes $\omega_i^n = 1 \, \forall i$ and n, the convergence of (the Gauß-Seidel type) algorithm (49)-(51) is guaranteed. However, as usual with this type of algorithm, it is always tempting to speed up the convergence through the use of $\omega_i^n > 1$, if feasible. In that direction, we suggest the following adaptive strategy for the choice of ω_i^n:

$$\text{If } (u_i^{n+1/2} - z_i)(u_i^n - z_i) \leq 0, \text{ take } \omega_i^n = 1, \text{ namely } u_i^{n+1} = u_i^{n+1/2}, \tag{55}$$

else

$$\text{if } \frac{u_i^{n+1/2} - z_i}{u_i^n - z_i} \geq 1, \text{ take } \omega_i^n = \omega_f \, (\text{with } \omega_f \in (1, \omega_{\text{opt}}]), \tag{56}$$

else (since $0 < (u_i^{n+1/2} - z_i)/(u_i^n - z_i) < 1$) take

$$\omega_i^n = \min \left(\frac{u_i^n - z_i}{u_i^n - u_i^{n+1/2}}, \omega_f \right). \tag{57}$$

In (56), ω_{opt} (< 2) is the *optimal relaxation parameter* for the solution of the linear systems associated to matrix $\boldsymbol{A}$. The choice of ω_f will be discussed in the following section.

4.3 Convergence of the relaxation algorithm

In this paragraph we are going to prove the convergence of the relaxation algorithm (49)-(51), assuming that ω_i^n is provided by (55)-(57). To prove the convergence, we will make a systematic use of the following classical relation (which is nothing but a Taylor expansion applied to the polynomial function $J_0(\cdot)$):

$$J_0(\boldsymbol{w}) - J_0(\boldsymbol{v}) = (\boldsymbol{A}\boldsymbol{v} - \boldsymbol{b}) \cdot (\boldsymbol{w} - \boldsymbol{v}) + \frac{1}{2} \boldsymbol{A}(\boldsymbol{w} - \boldsymbol{v}) \cdot (\boldsymbol{w} - \boldsymbol{v}), \, \forall \boldsymbol{v}, \boldsymbol{w} \in \mathbb{R}^n. \tag{58}$$

We are going to prove now the following *convergence theorem*

Theorem 4.1. *Suppose that we use* (55)-(57) *to adjust* ω_i^n. *Then,* $\forall \boldsymbol{u}^0 \in \mathbb{R}^N$, *we have*

$$\lim_{n\to+\infty} \boldsymbol{u}^n = \boldsymbol{u}, \tag{59}$$

$\boldsymbol{u}$ *being the solution of problem* (45), (48).

Proof. We divide the proof in two parts, the first one being dedicated to proving that if (55)-(57) holds, then

$$\lim_{n\to+\infty} (\boldsymbol{u}^{n+1} - \boldsymbol{u}^n) = \mathbf{0}. \tag{60}$$

1) We have

$$\begin{aligned} &J(\boldsymbol{u}^n) - J(\boldsymbol{u}^{n+1}) \\ &\quad = \sum_{i=1}^{N} [J(u_1^{n+1}, \dots, u_{i-1}^{n+1}, u_i^n, \dots, u_N^n) - J(u_1^{n+1}, \dots, u_{i-1}^{n+1}, u_i^{n+1}, u_{i+1}^n, \dots, u_N^n)] \\ &\quad = \sum_{i=1}^{N} [J_0(u_1^{n+1}, \dots, u_{i-1}^{n+1}, u_i^n, \dots, u_N^n) - J_0(u_1^{n+1}, \dots, u_{i-1}^{n+1}, u_i^{n+1}, u_{i+1}^n, \dots, u_N^n) \\ &\qquad\qquad + \alpha_i(|u_i^n - z_i| - \left|u_i^{n+1} - z_i\right|)] \end{aligned} \tag{61}$$

(i) Consider first those indices i for which (55) prevails; we have then $\omega_i^n = 1$ and $u_i^{n+1} = u_i^{n+1/2}$ and the corresponding terms in (61) verify from (58):

$$\begin{aligned} &J(u_1^{n+1}, \dots, u_{i-1}^{n+1}, u_i^n, \dots, u_N^n) - J(u_1^{n+1}, \dots, u_{i-1}^{n+1}, u_i^{n+1}, u_{i+1}^n, \dots, u_N^n) \\ &= J_0(u_1^{n+1}, \dots, u_{i-1}^{n+1}, u_i^n, \dots, u_N^n) - J_0(u_1^{n+1}, \dots, u_{i-1}^{n+1}, u_i^{n+1}, u_{i+1}^n, \dots, u_N^n) \\ &\quad + \alpha_i(|u_i^n - z_i| - \left|u_i^{n+1} - z_i\right|) \\ &= \frac{\partial J_0}{\partial u_i}(u_1^{n+1}, \dots, u_{i-1}^{n+1}, u_i^{n+1}, u_{i+1}^n, \dots, u_N^n)(u_i^n - u_i^{n+1}) \\ &\quad + \frac{1}{2} a_{ii} \left|u_i^n - u_i^{n+1}\right|^2 + \alpha_i(|u_i^n - z_i| - \left|u_i^{n+1} - z_i\right|). \end{aligned} \tag{62}$$

Since $u_i^{n+1} = u_i^{n+1/2}$ it follows from (52) and (55) that (62) reduces to

$$J(u_1^{n+1}, \dots, u_{i-1}^{n+1}, u_i^n, \dots, u_N^n) - J(u_1^{n+1}, \dots, u_{i-1}^{n+1}, u_i^{n+1}, u_{i+1}^n, \dots, u_N^n) \geq \frac{1}{2} a_{ii} \left|u_i^n - u_i^{n+1}\right|^2. \tag{63}$$

(ii) The other two situations, namely the ones associated with (56) and (57) are easier to handle since the mapping $v_i \mapsto J(u_1^{n+1}, \dots, u_{i-1}^{n+1}, v_i, u_{i+1}^n, \dots, u_N^n)$ is linear-quadratic when restricted to the half-lines $v_i \leq z_i$ and $v_i \geq z_i$, implying in particular that in the situations (56) and (57) we have

$$\frac{\partial J}{\partial u_i}(u_1^{n+1}, \dots, u_{i-1}^{n+1}, u_i^{n+1/2}, u_{i+1}^n, \dots, u_N^n) = 0 \tag{64}$$

since $u_i^{n+1/2} \neq z_i$; we also have

$$\frac{\partial J}{\partial u_i}(u_1^{n+1}, \dots, u_{i-1}^{n+1}, w_i, u_{i+1}^n, \dots, u_N^n) - \frac{\partial J}{\partial u_i}(u_1^{n+1}, \dots, u_{i-1}^{n+1}, v_i, u_{i+1}^n, \dots, u_N^n) = a_{ii}(w_i - v_i), \tag{65}$$

if v_i and w_i are on the same side of z_i (which is the case of $u_i^{n+1/2}$).

If (56) or (57) hold we have thus from (58), (64), and (65):

$$\begin{aligned}
&J(u_1^{n+1},\dots,u_{i-1}^{n+1},u_i^n,\dots,u_N^n)-J(u_1^{n+1},\dots,u_{i-1}^{n+1},u_i^{n+1},u_{i+1}^n,\dots,u_N^n)\\
&=\frac{\partial J}{\partial u_i}(u_1^{n+1},\dots,u_{i-1}^{n+1},u_i^{n+1},u_{i+1}^n,\dots,u_N^n)(u_i^n-u_i^{n+1})+\frac{1}{2}a_{ii}\left|u_i^n-u_i^{n+1}\right|^2\\
&=[\frac{\partial J}{\partial u_i}(u_1^{n+1},\dots,u_{i-1}^{n+1},u_i^{n+1},u_{i+1}^n,\dots,u_N^n)\\
&\quad-\frac{\partial J}{\partial u_i}(u_1^{n+1},\dots,u_{i-1}^{n+1},u_i^{n+1/2},u_{i+1}^n,\dots,u_N^n)](u_i^n-u_i^{n+1})+\frac{1}{2}a_{ii}\left|u_i^n-u_i^{n+1}\right|^2\\
&=a_{ii}(u_i^{n+1}-u_i^{n+1/2})(u_i^n-u_i^{n+1})+\frac{1}{2}a_{ii}\left|u_i^n-u_i^{n+1}\right|^2.
\end{aligned}\tag{66}$$

Observe that we have, from (51), $u_i^{n+1}-u_i^{n+1/2}=\frac{\omega_i^n-1}{\omega_i^n}(u_i^{n+1}-u_i^n)$ which combined with (66) yields

$$\begin{aligned}
&J(u_1^{n+1},\dots,u_{i-1}^{n+1},u_i^n,\dots,u_N^n)-J(u_1^{n+1},\dots,u_{i-1}^{n+1},u_i^{n+1},u_{i+1}^n,\dots,u_N^n)\\
&\qquad=\frac{2-\omega_i^n}{2\omega_i^n}a_{ii}\left|u_i^{n+1}-u_i^n\right|^2\geq\frac{2-\omega_f}{2\omega_f}a_{ii}\left|u_i^{n+1}-u_i^n\right|^2,
\end{aligned}\tag{67}$$

if (56) or (57) hold.

Since $\omega_f\in[1,2)$, we have $0<(2-\omega_f)/(2\omega_f)\leq 1$. Combining (63) and (67) we obtain by summation in i that

$$J(\boldsymbol{u}^n)-J(\boldsymbol{u}^{n+1})\geq\frac{2-\omega_f}{2\omega_f}\sum_{i=1}^N a_{ii}\left|u_i^{n+1}-u_i^n\right|^2.\tag{68}$$

It follows from (63) and (68) that the sequence $\{J(\boldsymbol{u}^n)\}_{n\geq 0}$ is decreasing; since it is bounded from below by $J(\boldsymbol{u})$, it converges to some limit, implying that the left and then right side in (68) converge to zero as $n\to+\infty$. We have thus proved (60) since $a_{ii}>0$, $\forall i=1,\dots,N$.

2) To prove the convergence of $\{\boldsymbol{u}^n\}_{n\geq 0}$, we observe that (48) implies

$$(\boldsymbol{A}\boldsymbol{u}-\boldsymbol{b})\cdot(\boldsymbol{u}^n-\boldsymbol{u})+\sum_{i=1}^N\alpha_i[|u_i^n-z_i|-|u_i-z_i|]\geq 0,$$

which implies in turn that

$$\begin{aligned}
&(\boldsymbol{A}\boldsymbol{u}^n-\boldsymbol{b})\cdot(\boldsymbol{u}^n-\boldsymbol{u})+\sum_{i=1}^N\alpha_i[|u_i^n-z_i|-|u_i-z_i|]\\
&\qquad=\sum_{i=1}^N\frac{\partial J_0}{\partial u_i}(\boldsymbol{u}^n)(u_i^n-u)+\sum_{i=1}^N\alpha_i[|u_i^n-z_i|-|u_i-z_i|]\geq\boldsymbol{A}(\boldsymbol{u}^n-\boldsymbol{u})\cdot(\boldsymbol{u}^n-\boldsymbol{u}).
\end{aligned}\tag{69}$$

It follows from (69) that

$$\sum_{i=1}^{N}[\frac{\partial J_0}{\partial u_i}(\boldsymbol{u}^n) - \frac{\partial J_0}{\partial u_i}(u_1^{n+1},\ldots,u_{i-1}^{n+1},u_i^{n+1/2},u_{i+1}^n,\ldots,u_N^n)](u_i^n-u_i)$$
$$+\sum_{i=1}^{N}\frac{\partial J_0}{\partial u_i}(u_1^{n+1},\ldots,u_{i-1}^{n+1},u_i^{n+1/2},u_{i+1}^n,\ldots,u_N^n)(u_i^n-u_i)+\sum_{i=1}^{N}\alpha_i[|u_i^n-z_i|-|u_i-z_i|]$$
$$\geq \boldsymbol{A}(\boldsymbol{u}^n-\boldsymbol{u})\cdot(\boldsymbol{u}^n-\boldsymbol{u}). \quad (70)$$

Relation (70) can be rewritten as

$$\sum_{i=1}^{N}[\sum_{j=1}^{i-1}a_{ij}(u_j^n-u_j^{n+1})+a_{ii}(u_i^n-u_i^{n+1/2})](u_i^n-u_i)$$
$$+\sum_{i=1}^{N}\frac{\partial J_0}{\partial u_i}(u_1^{n+1},\ldots,u_{i-1}^{n+1},u_i^{n+1/2},u_{i+1}^n,\ldots,u_N^n)(u_i^n-u_i^{n+1/2})+\sum_{i=1}^{N}\alpha_i[|u_i^n-z_i|-\left|u_i^{n+1/2}-z_i\right|]$$
$$\geq\sum_{i=1}^{N}\frac{\partial J_0}{\partial u_i}(u_1^{n+1},\ldots,u_{i-1}^{n+1},u_i^{n+1/2},u_{i+1}^n,\ldots,u_N^n)(u_i-u_i^{n+1/2})$$
$$+\alpha_i[|u_i-z_i|-\left|u_i^{n+1/2}-z_i\right|]+\boldsymbol{A}(\boldsymbol{u}^n-\boldsymbol{u})\cdot(\boldsymbol{u}^n-\boldsymbol{u}).$$

Since from (68) the sequence $\{J(\boldsymbol{u}_n)\}_{n\geq 0}$ is bounded, it implies that the sequence $\{\boldsymbol{u}_n\}_{n\geq 0}$ is bounded in $\mathbb{R}^N$. Moreover, (51) and (60) imply $\lim_{n\to+\infty}(\boldsymbol{u}^{n+1/2}-\boldsymbol{u}^n)=\boldsymbol{0}$. Combining these properties with the Lipschitz continuity of the function $\xi\to|\xi|$, we can easily show that the

$$\text{left-hand side of (70) converges to zero as } n\to+\infty. \quad (71)$$

Since, from (52), the first term in the right-hand side is ≥ 0, it follows from (70) and (71) that

$$\lim_{n\to+\infty}\boldsymbol{A}(\boldsymbol{u}^n-\boldsymbol{u})\cdot(\boldsymbol{u}^n-\boldsymbol{u})=0.$$

Matrix $\boldsymbol{A}$ being positive definite, the above relation implies $\lim_{n\to+\infty}\boldsymbol{u}^n=\boldsymbol{u}$, which completes the proof of the theorem. □

Remark 4.2 (On the choice of ω_f)**.** *Suppose that one applies algorithm* (49)-(51) *to the solution of problem* (1)*, using a single relaxation parameter ω, i.e., ω is independent of i and n. On one hand, for the Gauß-Seidel type method with $\omega=1$, we surely have convergence. On the other hand, for small h, ω_{opt} is close to 2. These observations together suggest that a universal candidate for optimal ω would be around 1.5. However, numerical tests suggest that better and sharper way is to majorize ω_i^n in* (56), (57) *by ω_{opt}.*

5 Solving problem (1) in $H^1(\Omega)$

5.1 Generalities

There is no basic difficulty at generalizing the methodology discussed in the previous sections to those cases where the set V in problem (1) is of the following type:

$$V = \{v \in H^1(\Omega), v = g \text{ on } \Gamma_0\}, \tag{72}$$

where Γ_0 is an open subset (not necessarily connected) of the boundary Γ of Ω (we have thus $\int_{\Gamma_0} d\Gamma > 0$); indeed, assuming that g is smooth enough (i.e., $\exists \tilde{g} \in H^1(\Omega)$ such that $g = \tilde{g}|_{\Gamma_0}$) the affine space V is non-empty implying that the associated problem (1) has a unique solution u verifying the variational inequality problem (2), with V replacing $H_0^1(\Omega)$. Similarly, the solution u of the prob1em (1), (72) is characterized by the following variant of system (4):

$$\begin{aligned}
&u \in V, \lambda \in \Lambda = \{\mu \in L^2(\Omega) \mid |\mu(x)| \leq 1, \text{ a.e. on } \Omega\},\\
&-\beta_1 \frac{\partial^2 u}{\partial x_1^2} - \beta_2 \frac{\partial^2 u}{\partial x_2^2} + \lambda = 0 \text{ in } \Omega,\\
&\bar{\bar{\beta}} \nabla u \cdot \boldsymbol{n} = 0 \text{ on } \Gamma \setminus \Gamma_0,\\
&\lambda(u - z) = |u - z|,
\end{aligned} \tag{73}$$

where, in (73), $\bar{\bar{\beta}}$ denotes the matrix $\begin{pmatrix} \beta_1 & 0 \\ 0 & \beta_2 \end{pmatrix}$ and $\boldsymbol{n}$ is the unit outward normal vector at Γ, i.e., u verifies a Neumann boundary condition on $\Gamma \setminus \Gamma_0$ and a Dirichlet one on Γ_0. As in Section 2 with (4), we can derive from (73) an Uzawa algorithm operating in $V \times \Lambda$ and converging to $\{u, \lambda\}$, if the analogue of ρ in algorithm (5)-(7), is taken positive and small enough. The finite element method discussed in Section 3 applies, after minor modifications, to the approximation of the problem (1), (72). To solve the resulting finite dimensional problem, we can use the relaxation method discussed in Section 4.

In this section we are going to address the case where in problem (1) we have:

$$V = H^1(\Omega). \tag{74}$$

Such a choice makes sense from a practical point of view; it avoids in particular the preprocessing of the boundary data as described in Section 6.1. From a mathematical point of view, problem (1) is a little more complicated with V defined by (74) than by (72), concerning in particular the uniqueness of the solution. This increase in complexity persists at the discrete level.

5.2 Formulation of the variational problem. Existence and uniqueness of solutions

With $\mathcal{J}(\cdot)$ still defined by

$$\mathcal{J}(v) = \int_\Omega \left[|v - z| + \frac{1}{2}\beta_1 \left| \frac{\partial v}{\partial x_1} \right|^2 + \frac{1}{2}\beta_1 \left| \frac{\partial v}{\partial x_2} \right|^2 \right] dx,$$

we consider the following problem from *Calculus of Variations*:

$$\text{Find } u \in H^1(\Omega) \text{ such that } \mathcal{J}(u) \leq \mathcal{J}(v), \forall v \in H^1(\Omega). \tag{75}$$

We will start our discussion on the existence of solutions to problem (75) by proving the following

Lemma 5.1. *The functional*

$$v \mapsto [\|v\|^2_{L^1(\Omega)} + \int_\Omega |\nabla v|^2 \, dx]^{1/2} \tag{76}$$

defines over $H^1(\Omega)$ a norm equivalent to the (usual) $H^1(\Omega)$-norm

$$v \mapsto [\|v\|^2_{L^2(\Omega)} + \int_\Omega |\nabla v|^2 \, dx]^{1/2}.$$

Proof. Let us denote by $|||\cdot|||$ the functional in (76); this functional is clearly a norm over $H^1(\Omega)$. Moreover, since Ω is bounded we have (from the Schwarz inequality in $L^2(\Omega)$)

$$\|v\|_{L^1(\Omega)} \leq |\Omega|^{1/2} \|v\|_{L^2(\Omega)}, \forall v \in L^2(\Omega) \, (\supset H^1(\Omega)), \tag{77}$$

with $|\Omega| = \text{measure}(\Omega)$. Combining (76) with (77) yields

$$|||v||| \leq \max(1, |\Omega|^{1/2}) \|v\|_{H^1(\Omega)}, \forall v \in H^1(\Omega). \tag{78}$$

Suppose that there is no positive constant γ such that

$$\|v\|_{H^1(\Omega)} \leq \gamma |||v|||, \forall v \in H^1(\Omega). \tag{79}$$

This implies the existence of a sequence $\{v_n\}_{n\geq 0}$ such that

$$v_n \in H^1(\Omega) \text{ with } \|v_n\|_{H^1(\Omega)} = 1, \forall n \geq 0, \tag{80}$$

$$\lim_{n\to+\infty} |||v_n||| = 0. \tag{81}$$

Relation (81) implies

$$\lim_{n\to+\infty} \|v_n\|_{L^1(\Omega)} = \lim_{n\to+\infty} \int_\Omega |\nabla v_n|^2 \, dx = 0. \tag{82}$$

Combining (80) with (82) yields

$$\lim_{n\to+\infty} \|v_n\|_{L^2(\Omega)} = 1. \tag{83}$$

The sequence $\{v_n\}_{n\geq 0}$ being *bounded* in (the Hilbert space) $H^1(\Omega)$, we can extract from it a subsequence – still denoted by $\{v_n\}_{n\geq 0}$ – such that

$$\lim_{n\to+\infty} v_n = w \text{ } \textit{weakly} \text{ in } H^1(\Omega). \tag{84}$$

Since Ω is bounded, it follows from the celebrated *Kondrachev theorem* (see, e.g., [17]) that the injection from $H^1(\Omega)$ into $L^2(\Omega)$ (and therefore into $L^1(\Omega)$) is compact. We have thus, from (84),

$$\lim_{n\to+\infty} v_n = w \text{ in } L^2(\Omega),$$

which combined with (82) and (83) yields

$$\|w\|_{L^1(\Omega)} = 0 \text{ and } \|w\|_{L^2(\Omega)} = 1. \tag{85}$$

The first relation in (85) implying $w = 0$, the second one makes no sense, which implies that sequences verifying (80) and (81) do not exist, which implies in turn the existence of $\gamma > 0$ such that relation (79) holds true. Inequalities (78) and (79) imply the equivalence of the two norms. □

Equipped with Lemma 5.1, we can easily prove the following

Theorem 5.1. *Suppose that $z \in L^2(\Omega)$; then, the variational problem* (75) *has at least one solution. Moreover, the solutions of problem* (75) *are characterized by*

$$u \in H^1(\Omega), \quad \int_\Omega \bar{\bar{\beta}}\nabla u \cdot \nabla(v-u)dx + j(v) - j(u) \geq 0, \forall v \in H^1(\Omega), \tag{86}$$

where

$$j(v) = \int_\Omega |v - z|\, dx, \forall v \in L^1(\Omega)(\supset H^1(\Omega)).$$

Proof. Observe that the functional $\mathcal{J}(\cdot)$ being *convex* and *continuous* over $H^1(\Omega)$ is *weakly lower semi-continuous* on that space. Next, consider a minimizing sequence $\{u_n\}_{n\geq 0}$ for problem (75); we have thus

$$\begin{array}{l} u_n \in H^1(\Omega), \forall n \geq 0, \text{ and} \\ \lim\limits_{n\to+\infty} \mathcal{J}(u_n) = \inf\limits_{v\in H^1(\Omega)} \mathcal{J}(v) \geq 0. \end{array} \tag{87}$$

We clearly have

$$\|u_n\|_{L^1(\Omega)} \leq C \text{ and } \int_\Omega |\nabla u_n|^2\, dx \leq C, \forall n \geq 0,$$

for some constant $C(> 0)$, which implies, from Lemma 5.1, that the sequence $\{u_n\}_{n\geq 0}$ is bounded in $H^1(\Omega)$. We can extract thus from $\{u_n\}_{n\geq 0}$ a subsequence – still denoted by $\{u_n\}_{n\geq 0}$ – such that

$$\lim_{n\to+\infty} u_n = u \textit{ weakly} \text{ in } H^1(\Omega).$$

From the *weak lower semi-continuity* property mentioned above, we have

$$\inf \mathcal{J}(v) \leq \mathcal{J}(u) \leq \liminf_{n\to+\infty} \mathcal{J}(u_n) = \lim_{n\to+\infty} \mathcal{J}(u_n) = \inf_{v\in H^1(\Omega)} \mathcal{J}(v),$$

a chain of relations showing that $\mathcal{J}(u) = \inf_{v\in H^1(\Omega)} \mathcal{J}(v)$.

Since $\mathcal{J}(\cdot) = \mathcal{J}_0(\cdot) + j(\cdot)$, where

$$\mathcal{J}_0(v) = \frac{1}{2}\int_\Omega \left[\beta_1 \left|\frac{\partial v}{\partial x_1}\right|^2 + \beta_2 \left|\frac{\partial v}{\partial x_2}\right|^2\right] dx \,(= \frac{1}{2}\int_\Omega \bar{\bar{\beta}}\nabla v \cdot \nabla v dx), \forall v \in H^1(\Omega),$$

the *variational inequality characterization* (86) follows classically (see, e.g., [3, Lemma I.4.1], [5]) from the *convexity* of $j(\cdot)$ and $\mathcal{J}_0(\cdot)$ and from the differentiability of $\mathcal{J}_0(\cdot)$. □

Now that the *existence* of solutions to problem (75) has been "secured", we are going to investigate the *uniqueness* (or *non-uniqueness*) properties of the solution(s). A first step in that direction is provided by the following

Theorem 5.2. *All the solutions to problem* (75) *have the same component in* $H^1(\Omega) \cap L^2_0(\Omega)$ *in the decomposition* $H^1(\Omega) = (H^1(\Omega) \cap L^2_0(\Omega)) \oplus \mathbb{R}$, *where* $L^2_0(\Omega) = \{v \in L^2(\Omega) \mid \int_\Omega v dx = 0\}$.

Proof. Suppose that both u_1 and u_2 are solutions to problem (75); it follows then from (86) that

$$\int_\Omega \bar{\bar{\beta}}\nabla u_1 \cdot \nabla(u_2 - u_1) dx + j(u_2) - j(u_1) \geq 0$$

and

$$\int_\Omega \bar{\bar{\beta}}\nabla u_2 \cdot \nabla(u_1 - u_2) dx + j(u_1) - j(u_2) \geq 0.$$

The above two relations imply by addition that

$$\min(\beta_1, \beta_2) \int_\Omega |\nabla(u_2 - u_1)|^2 \, dx \leq \int_\Omega \bar{\bar{\beta}}\nabla(u_2 - u_1) \cdot \nabla(u_2 - u_1) dx \leq 0,$$

which implies in turn that $\nabla(u_2 - u_1) = 0$ on Ω, i.e., $u_2 - u_1 =$ constant, which proves the theorem. □

In order to push our analysis further, we are going to take advantage of the fact that the solutions to problem (75) verify the following variant of the characterization (4) (which was obtained for $V = H^1_0(\Omega)$ in (1)):

$$\begin{aligned} &u \in V, \lambda \in \Lambda = \{\mu \in L^2(\Omega) \mid |\mu(x)| \leq 1 \text{ a.e. on } \Omega\}, \\ &-\beta_1 \frac{\partial^2 u}{\partial x_1^2} - \beta_2 \frac{\partial^2 u}{\partial x_2^2} + \lambda = 0 \text{ in } \Omega, \\ &\bar{\bar{\beta}}\nabla u \cdot \boldsymbol{n} = 0 \text{ on } \Gamma, \\ &\lambda(u - z) = |u - z|\,. \end{aligned} \tag{88}$$

It follows from (88) and classical regularity results for the solution of elliptic equations with constant coefficients (see, e.g., [17, 7]) that if Ω is convex and/or Γ smooth enough, then $u \in W^{2,p}(\Omega), \forall p \in [1, +\infty)$ (which implies that $u \in C^{1,\alpha}(\bar{\Omega}), \forall \alpha \in [0, +\infty)$, i.e., u has "almost" the $C^2(\bar{\Omega}$-regularity). Another implication of (88) and Theorem 5.2 is that *all* the solutions to problem (75) "share" the same λ. We are going to use the characterization (88) to identify a particular problem (75), which has multiple (in fact an infinity of) solutions if β_1 is *large enough*:

Take $\Omega = (-a, a) \times (0, b)$, where a and b are both positive, and z defined as follows:

$$z(x) = \begin{cases} 0, & \text{if } x \in (-a, 0) \times (0, b), \\ 1, & \text{if } x \in (0, a) \times (0, b). \end{cases} \tag{89}$$

Using (88), one easily verifies that the solutions of problem (75), (89) are given

(i) if $\beta_1 > a^2$, by

$$u(x_1, x_2) = u_0(x_1, x_2) + c, \forall \{x_1, x_2\} (= x) \in \Omega, \tag{90}$$

with

$$u_0(x_1, x_2) = \frac{1}{2} + \frac{1}{2\beta_1} x_1 (2a - |x_1|)$$

and

$$c \in \left[-\frac{1}{2}(1 - \frac{a^2}{\beta_1}), \frac{1}{2}(1 - \frac{a^2}{\beta_1}) \right].$$

Problem (75) has thus in *infinite* family of solutions parametrized by c if $\beta_1 > a^2$.

(ii) if $0 < \beta_1 \leq a^2$ by

$$u(x_1, x_2) = \begin{cases} 0 & \text{if } \{x_1, x_2\} \in (-a, -\sqrt{\beta_1}] \times (0, b) \\ \frac{1}{2} + \frac{1}{2\beta_1} x_1 (2\sqrt{\beta_1} - |x_1|), & \text{if } \{x_1, x_2\} \in [-\sqrt{\beta_1}, \sqrt{\beta_1}] \times (0, b), \\ 1 & \text{if } \{x_1, x_2\} \in [\sqrt{\beta_1}, a) \times (0, b). \end{cases} \tag{91}$$

Problem (75), (89) has thus a *unique* solution "as soon as" $0 < \beta_1 \leq a^2$.

The particular problem (75) that we are presently discussing is exemplary in the sense that z defined by (89) is a "pure" *jumping function* (clearly related to the *Heaviside step function*); it may be therefore instructive to study the behavior of u as $\boldsymbol{\beta} \to \mathbf{0}$. Taking advantage of the representation (91), we can easily show that

$$\|u - z\|_{L^1(\Omega)} = b\frac{\sqrt{\beta_1}}{3} \text{ and } \|u - z\|_{L^2(\Omega)} = \sqrt{b}\frac{\sqrt[4]{\beta_1}}{\sqrt{10}}. \tag{92}$$

To conclude this *uniqueness* related discussion we are going to complete Theorem 5.1 by proving the following

Theorem 5.3. *Suppose that $z \in C^0(\bar{\Omega})$; then the corresponding problem* (75) *has a unique solution.*

Proof. Observe first that it follows from (88) that

$$\int_\Omega \lambda dx = 0. \tag{93}$$

Suppose that (75) has a solution u such that $u - z \geq 0$. We have then, from (88), $\lambda(x) \geq 0$ a.e. on Ω, which combined with (93) implies $\lambda = 0$. It follows then from (88) that $u = z$. If w is also a solution of (75), it shares with u the same λ, implying, from (88), that $|w - z| = \lambda(w - z) = 0$. We have thus $w = z = u$, i.e., the uniqueness of the solution if $u - z \geq 0$.

A similar conclusion holds if $u - z \leq 0$. Suppose now that $u - z$ changes sign over Ω; since the functions u and z are both continuous, the sets $\Omega^+ = \{x \in \Omega \mid u(x) - z(x) > 0\}$ and $\Omega^- = \{x \in \Omega \mid u(x) - z(x) < 0\}$ are both open subsets of Ω. Suppose now that there exists a *positive* constant c such that $u + c$ is also a solution of (75). Take now $x_0 \in \partial\Omega^-$ (the boundary of Ω^-); we have then $u(x_0) - z(x_0) = 0$ and $u(x_0) + c - z(x_0) = c > 0$. From the continuity of the functions $u - z$ and $u + c - z$, there exists, "close to x_0", an open subset O of Ω^- such that $(u - z)|_O < 0$ and $(u + c - z)|_O > 0$. The first inequality implies, from (88), that $\lambda = -1$ on O, while the second inequality implies $\lambda = 1$ on O, which is contradictory, implying that there is no positive c such as $u + c$ solves (75). Using Ω^+ this time, we can prove similarly that there is no positive c such that $u - c$ solves (75); u is therefore the unique solution of (75). □

Remark 5.1. *This is the $H^1(\Omega)$ analogue of Remark 2.6: if u is the solution of* (75)*, we can prove that*

$$\lim_{\min\{\beta_1,\beta_2\}\to+\infty} = c_\infty \text{ in } W^{2,p}(\Omega), \forall p \in [1, +\infty),$$

the function function c_∞ being a constant*, solution to the following one-dimensional minimization problem:*

$$c_\infty \in \mathbb{R}, \quad \|z - c_\infty\|_{L^1(\Omega)} \leq \|z - c\|_{L^1(\Omega)}, \forall c \in \mathbb{R}.$$

Since the solution u to problem (75) *and c_∞ are not necessarily unique, the above convergence result has to be understood in the sense of sub-sequences.*

5.3 A brief discussion of the finite element approximation of problem (75)

We proceed as in Section 3, the main difference being that this time the fundamental discrete space is

$$V_h = \{v \in C^0(\bar{\Omega}) \mid v|_T \in P_1, \forall T \in \mathcal{T}_h\}, \tag{94}$$

with $\mathcal{T}_h$ a triangulation of Ω. From the set $\Sigma_k = \{P_i\}_{i=1}^{N_h}$ of the vertices of $\mathcal{T}_h$, we introduce the following vector basis of V_h:

$$\mathcal{B}_h = \{w_i\}_{i=1}^{N_h},$$

with w_i uniquely defined by

$$\forall i = 1, \ldots, N_h, w_i \in V_h, w_i(P_i) = 1, \quad w_i(P_j) = 0, \forall j = 1, \ldots, N_h, j \neq i.$$

We approximate problem (75) by

$$\text{Find } u_h \in V_h \text{ such that } J_h(u_h) \leq J_h(v), \forall v \in V_h, \tag{95}$$

where

$$J_h(v) = \frac{1}{2}\int_\Omega \left[\beta_1 \left|\frac{\partial v}{\partial x_1}\right|^2 + \beta_2 \left|\frac{\partial v}{\partial x_2}\right|^2\right] dx + \frac{1}{2}\sum_{i=1}^{N_h} \alpha_i \left|v(P_i) - z_i\right|, \tag{96}$$

with α_i as in Section 3.

We can "easily" prove the following

Theorem 5.4. *The finite dimensional problem* (95) *has at least one solution. Moreover, the solutions of* (95) *are characterized by*

$$\begin{aligned} &u_h \in V_h, \\ &\int_\Omega \left[\beta_1 \frac{\partial u_h}{\partial x_1}\frac{\partial (v-u_h)}{\partial x_1} + \beta_2 \frac{\partial u_h}{\partial x_2}\frac{\partial (v-u_h)}{\partial x_2}\right] dx \\ &\quad + \frac{1}{3}\left[\sum_{i=1}^{N_h} \alpha_i \left|v(P_i) - z_i\right| - \sum_{i=1}^{N_h} \alpha_i \left|u_h(P_i) - z_i\right|\right] \geq 0, \forall v \in V_h, \end{aligned} \tag{97}$$

and the existence of λ_h *such that*

$$\begin{aligned} &u_h \in V_h, \lambda_h \in \Lambda_h = \{\mu \in V_h \mid |\mu(P_i)| \leq 1, \forall i = 1, \ldots, N_h\}, \\ &\int_\Omega \left[\beta_1 \frac{\partial u_h}{\partial x_1}\frac{\partial v}{\partial x_1} + \beta_2 \frac{\partial u_h}{\partial x_2}\frac{\partial v}{\partial x_2}\right] dx + \frac{1}{3}\sum_{i=1}^{N_h} \alpha_i \lambda_h(P_i) v(P_i) = 0, \forall v \in V_h, \\ &\lambda_h(P_i)(u_h(P_i) - z_i) = \left|u_h(P_i) - z_i\right|, \forall i = 1, \ldots, N_h. \end{aligned} \tag{98}$$

Concerning the *uniqueness* property of the solutions to problem (95), we can show that, as in the continuous case, if u_h and u_h^* are both solutions of (95), then $u_h - u_h^*$ is a constant and moreover

$$\sum_{i=1}^{N_h} a_i \left|u_h(P_i) - z_i\right| = \sum_{i=1}^{N_h} a_i \left|u_h^*(P_i) - z_i\right|. \tag{99}$$

Suppose that u_h is a solution to (95) and introduce the sets I_+, I_0, and I_- defined by $I_+ = \{i \in \{1, \ldots, N_h\} \mid u_h(P_i) - z_i > 0\}$, $I_0 = \{i \in \{1, \ldots, N_h\} \mid u_h(P_i) - z_i = 0\}$, and $I_- = \{i \in \{1, \ldots, N_h\} \mid u_h(P_i) - z_i < 0\}$, respectively. Take now $c \in \mathbb{R}$, sufficiently small, so that $u_h(P_i) + c - z_i > 0$, $\forall i \in I_+$, and $u_h(P_i) + c - z_i < 0$, $\forall i \in I_-$. Suppose now that $u_h + c$ is also a solution to (95); it follows then from (99), and from the definition of I_+, I_0, and I_-, that

$$\begin{aligned} \sum_{i=1}^{N_h} \alpha_i \left|u_h(P_i) - z_i\right| &= \sum_{i=1}^{N_h} \alpha_i \left|u_h(P_i) + c - z_i\right| \\ &= \sum_{i\in I_+} \alpha_i (u_h(P_i) + c - z_i) + \sum_{i\in I_-} \alpha_i (z_i - c - u_h(P_i)) + |c| \sum_{i\in I_0} \alpha_i \\ &= c\Big(\sum_{i\in I_+} \alpha_i - \sum_{i\in I_-} \alpha_i\Big) + |c| \sum_{i\in I_0} \alpha_i + \sum_{i=1}^{N_h} \alpha_i \left|u_h(P_i) - z_i\right|. \end{aligned} \tag{100}$$

It follows from (99) and (100) that $u_h + c$ is a solution to (95) if and only if

$$c\Big(\sum_{i\in I_+} \alpha_i - \sum_{i\in I_-} \alpha_i\Big) + |c| \sum_{i\in I_0} \alpha_i = 0. \tag{101}$$

It is pretty obvious that equation (101) has non-trivial solutions if and only if

$$\left|\sum_{i\in I_+} \alpha_i - \sum_{i\in I_-} \alpha_i\right| = \sum_{i\in I_0} \alpha_i. \tag{102}$$

We have shown thus that if u_h is a solution to (95), other solutions (in fact an infinity of them) exist if and only if relation (102) holds.

Concerning the convergence of $\{u_h\}_h$ when $h \to 0$, it can proved, using the methods discussed in, e.g., [3, 5], that if the angles of the triangulation $\mathcal{T}_h$ are bounded from below, uniformly in h by $\theta_0 > 0$, then we can extract from $\{u_h\}_h$ sub-sequences converging in $H^1(\Omega)$ to solutions of problem (75). Actually, any converging sub-sequence extracted from $\{u_h\}_h$ converges (strongly in $H^1(\Omega)$) to a solution of problem (75).

There is more to say about the approximate problem (95), particularly its iterative solution; this will be discussed in a forthcoming publication. We will conclude this section by proving that if h being fixed, $\boldsymbol{\beta}$ is small enough, then $u_h = z_h$. In order to prove this result, we will start from (98), rewritten in vector-matrix form, using the notation of Section 3, Remarks 3.2 and 3.3; we have thus

$$\begin{aligned} &(\beta_1 \boldsymbol{A}_1 + \beta_2 \boldsymbol{A}_2)\boldsymbol{u} \cdot \boldsymbol{v} + \boldsymbol{D}\boldsymbol{\lambda} \cdot \boldsymbol{v} = 0, \\ &\lambda_i(u_i - z_i) = |u_i - z_i|\,, \forall i = 1, \ldots, N_h. \end{aligned} \tag{103}$$

In (103), the matrices $\boldsymbol{A}_1$, $\boldsymbol{A}_2$ are symmetric and positive definite, and $\boldsymbol{D}$ is the $N_h \times N_h$ diagonal matrix defined by $d_{ii} = \alpha_i$. Taking $\boldsymbol{v} = \boldsymbol{u} - \boldsymbol{z}$ in (103), we obtain

$$\begin{aligned} (\beta_1 \boldsymbol{A}_1 + \beta_2 \boldsymbol{A}_2)(\boldsymbol{u} - \boldsymbol{z}) \cdot (\boldsymbol{u} - \boldsymbol{z}) + \sum_{i=1}^{N_h} \alpha_i |u_i - z_i| &= -(\beta_1 \boldsymbol{\alpha}_i + \beta_2 \boldsymbol{A}_2)\boldsymbol{z} \cdot (\boldsymbol{u} - \boldsymbol{z}) \\ &\leq |\boldsymbol{\beta}| \sqrt{\|\boldsymbol{A}_1 \boldsymbol{z}\|_\infty^2 + \|\boldsymbol{A}_2 \boldsymbol{z}\|_\infty^2} \sum_{i=1}^{N_h} |u_i - z_i|\,, \end{aligned}$$

which implies in turn that

$$(\beta_1 \boldsymbol{A}_1 + \beta_2 \boldsymbol{A}_2)(\boldsymbol{u} - \boldsymbol{z}) \cdot (\boldsymbol{u} - \boldsymbol{z}) + \sum_{i=1}^{N_h} \left(\alpha_i - |\boldsymbol{\beta}| \sqrt{\|\boldsymbol{A}_1 \boldsymbol{z}\|_\infty^2 + \|\boldsymbol{A}_2 \boldsymbol{z}\|_\infty^2} \right) |u_i - z_i| \leq 0. \tag{104}$$

Suppose that

$$|\boldsymbol{\beta}| < (\min_{i=1,\ldots,N_h} \alpha_i) / \sqrt{\|\boldsymbol{A}_1 \boldsymbol{z}\|_\infty^2 + \|\boldsymbol{A}_2 \boldsymbol{z}\|_\infty^2}; \tag{105}$$

it follows then from (104) that $\boldsymbol{u} = \boldsymbol{z}$ if relation (105) holds. The right-hand side in (105) depends of the regularity of z; it ranges from $O(h^4)$ if z is piecewise continuous, to $O(1)$ if $z \in W^{2,\infty}(\Omega)$.

6 Numerical experiments

In this section, we present the results of numerical experiments. The experiments were performed on an HP9000/J280 workstation (180 MHz PA8000 CPU) and the 1-d and 2-d variants of (49)–(51) as part of Algorithm 2 were implemented with *C* language. As middleware for preparing the examples, calling the external C-routines and illustrating the results we used *Matlab*.

6.1 The denoising algorithm

To summarise the algorithmic results of earlier sections, the *nonsmooth* SOR (NSOR) algorithm for solving (43) reads as follows:

Algorithm 1. *Iterate* (49)–(51)*, where* $\boldsymbol{A} = \beta_1 \boldsymbol{A}_1 + \beta_2 \boldsymbol{A}_2$ *and* $u_i^{n+1/2}$ *and* ω_i^n *are computed using* (53) *and* (55)–(57)*, respectively, until*

$$\left\| \boldsymbol{u}^{k+1} - \boldsymbol{u}^k \right\|_\infty < \varepsilon. \tag{106}$$

Here ε *is a given stopping tolerance.*

In practice, in the light of Remark 4.1 (cf. also Section 5.1), we consider the nonhomogeneous Dirichlet boundary condition. Our overall suggestion for a denoising algorithm treats a two dimensional image data by first applying the technique of Section 4.2 on the boundary, which is supposed to consist of individual strips, i.e. $\partial\Omega = \cup_i \Gamma_i,\ i = 1, \ldots, n$. For example, for $\Omega = (x_0, x_1) \times (y_0, y_1)$ the natural division consists of $\Gamma_1 = (x_0, x_1) \times y_0$, $\Gamma_2 = (x_0, x_1) \times y_1$, $\Gamma_3 = x_0 \times (y_0, y_1)$, and $\Gamma_4 = x_1 \times (y_0, y_1)$. The presmoothed values at the boundaries are then used as a nonhomogeneous boundary condition in (43).

Algorithm 2.

0^o **Initialization:** *Choose* $\beta_1, \beta_2 > 0$ *and* $\omega_f \in (1, 2)$.

1^o **Boundary fix:** *Solve the one-dimensional counterpart of* (1) *using Algorithm 1 separately on the boundary strips* Γ_i *such that the change points between the strips are used as a nonhomogenous boundary condition in the individual problems. Here one needs to choose an appropriate single regularization parameter* $\tilde{\beta}$*, whose relation to* β_1, β_2 *depends on the application*[1]*. For example,* $\tilde{\beta} = 30 \max(\beta_1, \beta_2)$ *was applied in Figure 1 after some test runs.*

2^o **Domain fix:** *Solve the 2-d problem* (43) *using Algorithm 1 with the values from Step* 1 *determining the nonhomogeneous Dirichlet boundary condition.*

6.2 Comparison of restoration capability

As already mentioned in the introduction, the characteristic behaviour of the L_1 method (1) itself was thorouhly studied in [11] using simulated data and different analytical error measures. Here, we first continue the exploration of such a denoising methodology by introducing a brief comparison concerning the restoration properties of this method and a few well-known, popular methods, based on real data related to the front propagation process as presented in Section 1 (cf. Figure 1).

The denoising comparison is based on (pieces of) two samples from the burning front image repository that has been collected as part of the research activities. These two different sample images (data) are used in the following roles:

[1]Discretized two-dimensional problems have more supporting pixels for the unknown pointwise value to be determined than in the corresponding one dimensional case (see, e.g., [12]): typically such a shortage of information must be compensated with larger regularization parameter in 1-d for appropriate results.

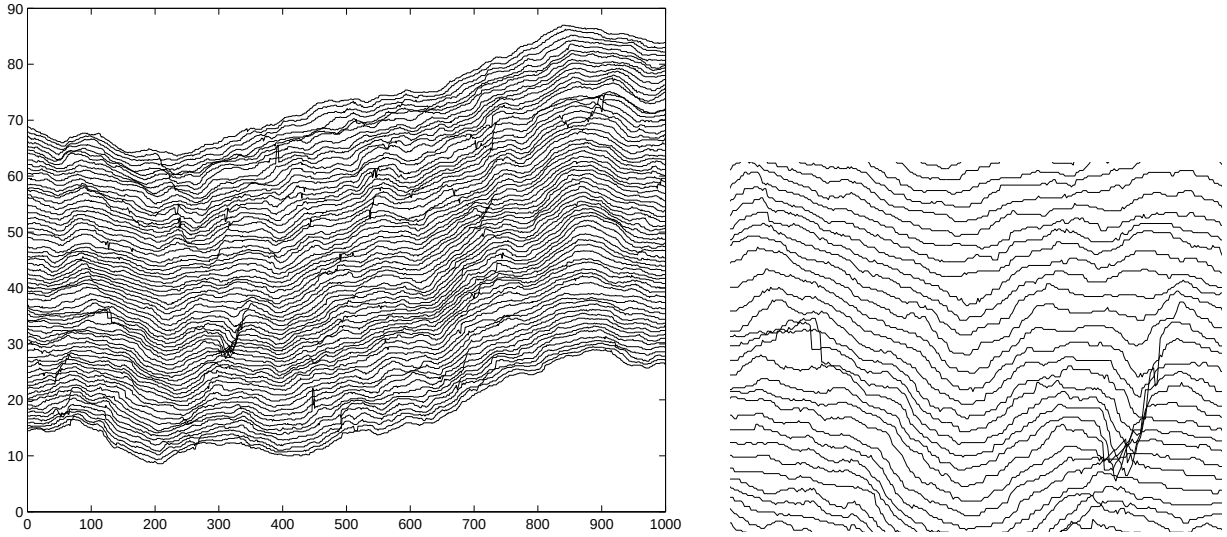

Figure 2: Test data image (left) and a local zoom (right).

1. **Test data:** The first image, illustrated in Figure 2, is used to fix the free parameters in different denoising methods to be tested (cf. Table 1). The image contains first seventy (70) burning fronts of an experiment.

2. **Validation data:** A second image is used to validate the results of different methods, which are illustrated in the figures given in Appendix B (cf. Table 2). We also used seventy (70) burning fronts from the initial image.

The two main goals and corresponding measures for denoising properties are the following:

Errors: The height of the propagating burning front should not decrease. To quantify this, we calculate the number of points (pixels) in an image $h \in R^{m\times n}$, where $h(t_i, x_j)+tol < h(t_{i-1}, x_j)$. Here t_i denotes the ith front, $i = 2, \ldots, m$, $(m = 70)$ and x_j the jth pixel $j = 1, \ldots, n$, $(n = 1000)$. *tol* denotes the tolerance related to the accumulation of floating point errors, which was taken as $10^5 \cdot machine\_epsilon \sim 10^{-11}$.

Distances: The local variation of the front shoud not be destroyed, i.e., the denoised image should be as close as possible to the original one excluding the outlying values with decreasing front. Moreover, to have a quantified possibility to compare the results of different methods, we also need a distance measure between their results. For this purpose, we compute the mean absolute deviation between two images (matrices) h_1 and h_2 according to

$$\frac{1}{n\,m}\sum_{i=1}^{m}\sum_{j=1}^{n}|(h_1)_{ij} - (h_2)_{ij}|.$$

Let us next describe shortly the methods that are to be compared with the one considered in this paper. Basically there exists numerous methods for image denoising and different classifications of possible techniques can be given. One way to classify different possibilities (cf., e.g., [14] and references therein) is to consider:

Transform based methods, where the basic idea is to, first, make a linear transformation of the given image (signal) to new basis, then decrease or remove the effect of coefficients corresponding to "noisy" basis functions, and, finally, reconstruct the denoised signal using the inverse transform with the modified coefficients/basis functions. Two of the most popular methods from this family were chosen, namely the Fourier method, where the transform is made to the frequency domain, and the Wavelet method where the time-frequency (scale) domain is considered [15]. We further restrict ourselves to one-dimensional methods, which are applied in a front-by-front fashion to raw images. Free parameters for the Fourier method is to decide which frequency band is diminished to suppress the noise, and for the Wavelet method to determine how the coefficients in the time-frequency plane should be modified.

Kernel based methods, where the basic idea is to define a local kernel (usually a moving window), which localizes the computation of a suitable statistical estimate representing the local reconstruction of a noisy pixel value. Two of the most popular methods from this family were chosen, namely the mean and median filter [6]. These methods become well-defined as soon as the shape of the moving window, here the length and hight of it in pixels, is given. Notice that pixels near the boundaries, where the mask refers to nonexisting values, need a special treatment. Here we choose the simplest solution to include in the computation of the estimate only those values that actually exist in the image.

Optimization/PDE based methods, where the basic idea is to define a suitable cost functional (or a PDE usually representing optimality condition of the corresponding cost functional), whose minimizer represents the smoothed image. The method considered in this paper, clearly, belongs to this class. The free parameters to be fixed (cf. Algorithm 2) are $\beta_1, \beta_2 > 0$, $\tilde{\beta} = f(\beta_1, \beta_2)$, and $\omega \in [1, 2)$.

Tables 1 and 2 in Appendix A contain the results (i.e., the errors and distances between different reconstructions) of different methods for test and validation images, respectively. The test data was used for hand-tuning the free parameters in different methods in such a way that the unphysical errors of decreasing front in the test image were removed completely. In practice, this yielded the following choices for different methods

Fourier: We used the *middle-band-rejection strategy* (see [20]), i.e. altogether 2.2% of the tails of the frequency band (11 lowest and 11 highest) was kept and the middle-band omitted.

Wavelet: We used 10th order Daubechies wavelet family with six levels of details (i.e. seven decomposition levels altogether). The wavelet coeffients $\{c_{lj}\}, l = 0, \ldots, 6, j = 0, \ldots, 1024$, were modified using *soft, adaptive thresholding strategy* (see [15, Chapter 10]), i.e.

$$c_{lj} = \begin{cases} \operatorname{sign}(c_{lj})\,(|c_{lj}| - \theta_l), & |c_{lj}| \geq \theta_l, \\ 0, & |c_{lj}| < \theta_l. \end{cases}$$

The levelwise thresholds $\{\theta_l\}$ were chosen as $\theta_{max} \cdot$ [0.01 0.02 0.03 0.04 0.05 0.05 0.01] where $\theta_{max} = \max_{lj} |c_{lj}|$.

Mean and Median: 5x7 window (mask) size was used for both approaches.

L_1-method: The parameters were chosen as $\beta_1 = 0.1,\ \beta_2 = \frac{\beta_1}{2},\ \tilde{\beta} = 30\beta_1$ for $\Gamma_1 \cup \Gamma_2$ (the x-boundary strips) and $\tilde{\beta} = 30\beta_2$ for $\Gamma_3 \cup \Gamma_4$ (the y-boundary strips).

Figures 5-9 show the actual appearance of the results of different methods for the validation image. Both the whole result (i.e., the restored image) and a zoomed, local result are given to illustrate the characteristic (qualitative) behavior of different methods.

Let us draw the following conclusions from these tests

- According to Tables 1 and 2 a cluster of quantitatively appropriate results (emphasized with bold font in the tables) is given by median filter and L_1 method. They both remove almost all errors and remain sufficiently close to each other and the original image. This result coincides with the basic charasteristic of the L_1-norm based M-estimate, the median, which can tolerate up to 50% of erroneous values [8]. As we see this behaviour is also captured in the L_1 method, which on the contrary to the local, window-based median also smooths the overall appearance of the image due to H^1 smoothing. The smoothing effect is also supported by the closeness of distances between the restorations of the mean filter and the L_1 method. The plain median filter, due to the discontinous character of the used statistical estimate, yields a staircase-like structure along the front lines. This (qualitative) difference is clearly visible in Figures 8 (right) and 9 (right).

- The transform-based, linear methods dramatically oversmooth the results and are unable to generalize the removal of erroneous values to the validation image. Also the mean filter yields some loss of details although the errors are well restored also in the validation image.

6.3 Efficiency of NSOR

Next we consider the efficiency of nonsmooth SOR. Three different strategies for choosing the over-relaxation parameter ω were tested and compared. The first approach (NSOR_fix) is to use a constant value ($\omega = 1$ or $\omega = 1.5$). The other approach (NSOR_var) is to have a variable choice according to (51). To this end, we also included in the comparison a simple adaptive approach (NSOR_ada), based on our numerical experience with NSOR. The heuristic is based on the general observation that ω should be as large as possible within the "convergence region" of the procedure. Hence, we start with a sufficient large value (1.6-1.7 was used in the numerical experiments) and if the error tolerance in (106) $e^{k+1} = \|u^{k+1} - u^k\|_\infty$ starts to increase, i.e. $e^{k+1} > e^k$ for $k \geq 1$, during the iterations (suggesting that the algorithm might be diverging), we decrease the current value of ω by taking 0.97ω.

To compare the efficiency of different approaches, we use the whole recordings of same two sample images as in the previous section, and study the number of iterations and the actual CPU time. Notice, however, that because the CPU time is measured from Matlab (tic...toc), the approach with varying ω_i^n is not comparable with the other approaches. It's

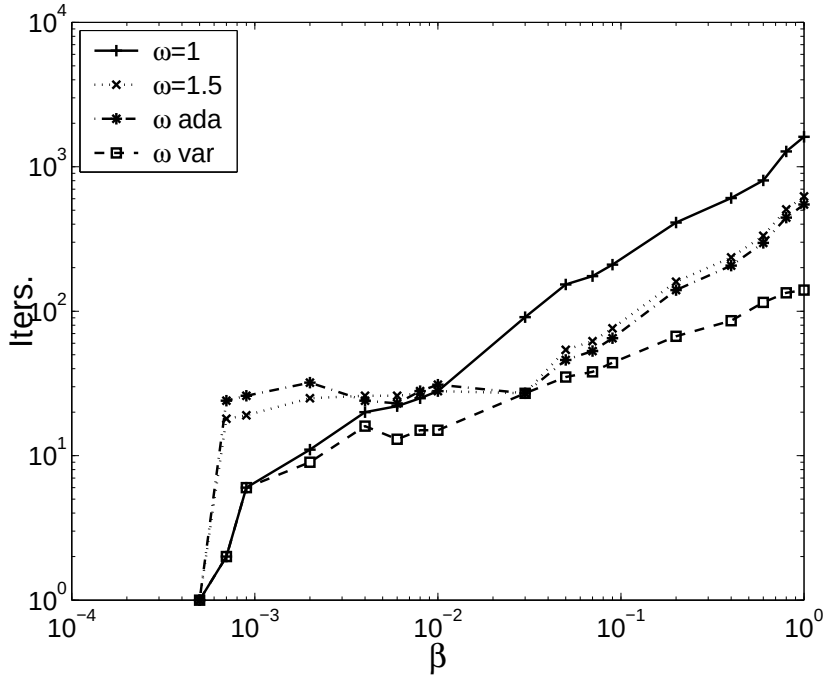

Figure 3: Number of iterations over different values of $\beta_1 \equiv \beta_2$ in Tables 5-7 for **Image 2** on logarithmic scales.

CPU time per iteration is much larger, because it includes transform of the over-relaxation vector $\{\omega_i^n\}_{i=1}^N$ between Matlab and the C-routines via the Mex-interface, which according to the numerical results seems to dominate the CPU usage. Hence, only number of iterations allows a true comparison between the efficiency of the scalar and vector-valued over-relaxation cases.

The results of these tests are reported in Tables 3-7 and illustrated in Figure 3. Based on all this information we draw the following conclusions:

Convergence and comparison of variants: All three variants and four actual procedures are able to solve the minimization problem and, from the denoising point of view, they all work very well in the appropriate region of the values of $\beta_1,\ \beta_2$. Furthermore, as illustrated in Figure 3, for small values of β the Gauss-Seidel type algorithm with $\omega = 1$ is very efficient, but its efficiency decreases dramatically as β increases. Both fixed over-relaxation $\omega = 1.5$ and the adaptive procedure stabilize the performance of the method over a large interval of possible values of the regularization parameter. As a whole, however, the most stable and efficent method is the one with varying ω_i^n, whose convergence was also thoroughly analyzed in Section 4.3, because its number of iterations both with respect to the number of unknowns (Tables 3–4) and different values of regularization parameters (Tables 5–7) remains in the best overall level.

Overall efficiency: From the computational point of view, the nonsmooth SOR algorithm is simpler but much more efficient and memory friendly than, e.g., the algorithm presented in [11]. More precisely, in the current implementation which is suitable for real images the elements of the FE representations $\mathbf{A}_1, \mathbf{A}_2$, and $\{\alpha_i\}_{i=1}^{N_{0h}}$ are included in

the procedure explicitly. This means that we do not need to allocate *any* additional vectors in the code, since pointwise updates to $\{u_i\}$ (and $\{\omega_i\}$ for NSOR_var) and also the monitoring of the error criterion can be implemented in an override fashion. Moreover, this means that the number of iterations of the algorithm coincides precisely with the number of sweeps through the data vectors. We feel that the efficiency of the proposed methodology is very promising, especially, when noticing that we are solving a nonsmooth optimization problem.

Effect of regularization: The algorithms are working better for smaller values of β_1, β_2, where the nonsmooth term in the cost functional is more dominating. Moreover, as illustrated in Table 6, too small values of the regularization parameters, where the formulation will not change the observation z at all, are indicated by only one iteration. This coincides with the analysis in Section 3 (Remarks 3.1 and 3.3) Hence, this allows one to tune and monitor the appropriate values of $\beta_i,\ i = 1, 2$, using visual inspection or, e.g., the heuristics proposed in [11, 1].

6.4 Conclusions from the numerical experiments

As a whole, we obtained very promising results from all the tests that were performed. The nonsmooth SOR procedure is simple to implement and it provides very efficient performance with minimal memory consumption. Hence, it is a very good candidate for even larger problems (with millions of pixels) where the overall smoothness is to be preserved, like in our lens-paper burn example.

Acknowledgements

The authors would like to thank the collaborators from the Department of Physics at the University of Jyväskylä (especially Dr. Maunuksela, Prof. Timonen, and Dr. Merikoski) for collecting the data and pointing out the basic challenges to be adressed. The help of post-graduate student Antti Vuorenmaa is also acknowledged for preparing the comparison of different methods. This work has been supported by the Academy of Finland and Technical Research Center of Finland (TEKES).

References

[1] J.-F. Aujol, G. Gilboa, T. Chan, and S. Osher, *Structure-texture image decomposition – modeling, algorithms, and parameter selection*, International Journal of Computer Vision, 67 (2006), pp. 111–136.

[2] J. Cea and R. Glowinski, *Sur des méthodes de minimisation par relaxation*, Revue Française d'Automatique, Informatique, Recherche Opérationnelle, Série Rouge, (1973), pp. 5–32.

[3] R. Glowinski, *Numerical Methods for Nonlinear Variational Problems*, Springer-Verlag, New York, 1984.

[4] R. Glowinski, *Finite element methods for incompressible viscous flow*, in Numerical Methods for Fluids, Part 3, vol. IX of Handbook of Numerical Analysis, North-Holland, 2003, pp. 3–1176.

[5] R. Glowinski, J. Lions, and R. Trémolières, *Numerical Analysis of Variational Inequalities*, North-Holland, Amsterdam, 1981.

[6] R. C. Gonzalez and R. E. Woods, *Digital Image Processing*, Addison-Wesley, 1993.

[7] P. Grisvard, *Elliptic Problems in Non-smooth Domains*, Pitman, 1985.

[8] P. J. Huber, *Robust Statistics*, Wiley series in probability and mathematical statistics, John Wiley & Sons, New York, 1981.

[9] A. K. Jain, *Fundamentals of Digital Image Processing*, Prentice-Hall, 1989.

[10] M. Kardar, G. Parisi, and Y.-C. Zhang, *Dynamic scaling of growing interfaces*, Phys. Rev. Letters, 56 (1986), pp. 889–892.

[11] T. Kärkkäinen, K. Kunisch, and K. Majava, *Denoising of smooth images using L^1-fitting*, Computing, 74 (2005), pp. 353–376.

[12] T. Kärkkäinen, K. Kunisch, and P. Tarvainen, *Augmented Lagrangian active set methods for obstacle problems*, Journal of Optimization Theory and Applications, 119 (2003), pp. 499–533.

[13] T. Kärkkäinen and J. Toivanen, *Building blocks for odd-even multigrid with applications to reduced systems*, Journal of Computational and Applied Mathematics, 131 (2001), pp. 15–33.

[14] K. Majava, *Optimization-Based Techniques for Image Restoration*, PhD dissertation, University of Jyväskylä, Department of Mathematical Information Technology, 2001.

[15] S. Mallat, *A Wavelet Tour of Signal Processing*, Academic Press, 1999.

[16] J. Maunuksela, M. Myllys, J. Merikoski, J. Timonen, T. Kärkkäinen, M. Welling, and R. Wijngaarden, *Determination of the stochastic evolution equation from noisy experimental data*, The European Physical Journal B, 33 (2003), pp. 193–202.

[17] J. Nečas, *Les méthodes directes en théorie des équations elliptiques*, Masson, 1967.

[18] M. Nikolova, *Minimizers of cost-functions involving nonsmooth data-fidelity terms. Application to the processing of outliers*, SIAM J. Numer. Anal., 40 (2002), pp. 965–994.

[19] C. R. Rao, *Methodology based on the L_1-norm, in statistical inference*, Sankhya: The Indian Journal of Statistics, 50 (1988), pp. 289–313.

[20] S. W. Smith, *The Scientist and Engineer's Guide to Digital Signal Processing*, California Technical Publishing, 1997.

[21] T. Valkonen, *Convergence of a SOR-Weiszfeld type algorithm for incomplete data sets*, Numerical Functional Analysis and Optimization, 27 (2006), pp. 931–952.

A Tables

	Errors	**Distances**				
		Fourier	Wavelet	Mean	Median	L_1
Original	373	0.5003	0.3796	0.1637	**0.0104**	**0.0683**
Fourier	0		0.4095	0.4872	0.4972	0.4844
Wavelet	0			0.3645	0.3765	0.3629
Mean	0				0.1583	**0.0983**
Median	0					**0.0658**
L_1	0					

Table 1: Errors and distances between the results of different methods for the test data image.

	Errors	**Distances**				
		Fourier	Wavelet	Mean	Median	L_1
Original	922	0.3147	0.3693	0.1950	**0.0266**	**0.0918**
Fourier	196		0.2967	0.2910	0.3062	0.2830
Wavelet	255			0.3409	0.3634	0.3400
Mean	16				0.1781	0.1094
Median	6					**0.0824**
L_1	3					

Table 2: Errors and distances between the results of different methods for the validation data image.

			Image 1			**Image 2**		
m	n	$m*n$	Iters.	CPU	ω	Iters.	CPU	ω
50	25	1 250	22	0.03	1.4603	26	0.01	1.4603
100	50	5 000	29	0.02	1.5054	30	0.02	1.5054
150	75	11 250	32	0.05	1.5520	30	0.05	1.5054
200	100	20 000	32	0.08	1.5520	34	0.09	1.5520
250	125	31 250	29	0.12	1.5054	34	0.14	1.4603
300	150	45 000	36	0.22	1.5520	45	0.27	1.4603
350	175	61 250	39	0.33	1.5520	35	0.29	1.5520
400	200	80 000	40	0.46	1.5054	43	0.49	1.5520
450	225	101 250	37	0.55	1.5520	73	1.05	1.5054
500	250	125 000	37	0.69	1.5520	64	1.18	1.5520
550	275	151 250	61	1.38	1.4603	62	1.41	1.5520
600	300	180 000	53	1.42	1.5054	64	1.75	1.5520
650	325	211 250	53	1.68	1.5054	62	2.15	1.5520
700	350	245 000	46	1.70	1.5520	64	2.47	1.5520
750	375	281 250	53	2.22	1.5054	64	2.68	1.5520
800	400	320 000	42	2.05	1.5520	73	3.65	1.5054
850	425	361 250	53	2.94	1.5054	64	3.56	1.5520
900	450	405 000	53	3.33	1.5054	64	4.10	1.5520
950	475	451 250	53	3.78	1.5054	62	4.67	1.5520
1000	500	500 000	53	4.49	1.5054	64	5.26	1.5520

Table 3: Number of iterations, CPU time, and final value of ω for NSOR_ada with, from the restoration result point of view, good values $\beta_1 = 0.2$ and $\beta_2 = 0.04$; $\varepsilon = 1e-5$ and $\omega^0 = 1.6$.

			Image 1		**Image 2**	
m	n	$m*n$	Iters.	CPU	Iters.	CPU
50	25	1 250	27	1.27	32	1.27
100	50	5 000	33	1.26	36	1.30
150	75	11 250	33	1.30	36	1.28
200	100	20 000	33	1.36	36	1.36
250	125	31 250	33	1.45	36	1.47
300	150	45 000	37	1.63	36	1.61
350	175	61 250	38	1.83	36	1.75
400	200	80 000	38	1.96	37	1.96
450	225	101 250	38	2.20	56	2.64
500	250	125 000	38	2.42	56	2.93
550	275	151 250	41	2.97	56	3.28
600	300	180 000	41	3.04	56	3.70
650	325	211 250	41	3.43	56	4.18
700	350	245 000	41	3.76	56	4.74
750	375	281 250	41	4.10	56	5.11
800	400	320 000	41	4.59	56	5.70
850	425	361 250	41	4.92	56	6.25
900	450	405 000	41	5.36	56	6.87
950	475	451 250	41	5.95	56	7.74
1000	500	500 000	41	6.46	56	8.29

Table 4: Same as Table 3, but using NSOR_var; $\omega_{Opt} = 1.6$.

	Image 1				**Image 2**			
	$\omega = 1$		$\omega = 1.5$		$\omega = 1$		$\omega = 1.5$	
β_1	Iters.	CPU	Iters.	CPU	Iters.	CPU	Iters.	CPU
5e-4	1	0.15	1	0.10	1	0.10	1	0.11
7e-4	2	0.18	17	1.17	2	0.19	18	1.22
9e-4	7	0.48	19	1.26	6	0.42	19	1.26
2e-3	10	0.71	26	1.80	11	0.76	25	1.69
4e-3	17	1.13	26	1.73	20	1.31	26	1.71
6e-3	18	1.24	27	1.94	22	1.50	26	1.77
8e-3	21	1.39	26	1.71	25	1.64	27	1.77
1e-2	28	2.03	27	1.88	28	1.90	28	1.91
3e-2	65	4.99	32	2.25	91	7.05	27	1.92
5e-2	108	9.44	33	2.49	153	13.14	54	4.20
7e-2	200	17.72	70	5.66	175	15.14	62	4.75
9e-2	208	19.12	73	5.91	210	18.73	76	6.05
2e-1	324	29.54	126	10.15	411	37.38	160	13.56
4e-1	764	68.77	293	25.36	607	55.89	236	20.31
6e-1	1193	104.67	457	40.24	804	71.96	333	28.43
8e-1	1616	132.57	636	60.28	1276	113.78	507	43.86
1	2104	178.14	840	71.81	1610	141.71	623	54.84

Table 5: Number of iterations and CPU time for NSOR_fix with different values of $\beta_1 \equiv \beta_2$; two fixed values of ω for $\varepsilon = 1e-5$, largest 1000x500 images from Table 3.

	Image 1			**Image 2**		
β_1	Iters.	CPU	ω	Iters.	CPU	ω
5e-4	1	0.10	1.6000	1	0.10	1.6000
7e-4	20	1.16	1.5520	24	1.56	1.6000
9e-4	27	1.63	1.6000	26	1.54	1.6000
2e-3	26	1.53	1.5054	32	2.08	1.6000
4e-3	36	2.20	1.6000	24	1.43	1.4603
6e-3	24	1.42	1.4603	23	1.52	1.4603
8e-3	30	1.83	1.5520	28	1.67	1.5054
1e-2	31	1.85	1.5520	31	2.04	1.5520
3e-2	32	2.14	1.4603	27	1.79	1.5054
5e-2	33	2.34	1.5054	46	3.48	1.5520
7e-2	69	5.52	1.5054	53	4.12	1.5520
9e-2	72	5.97	1.5054	65	5.43	1.5520
2e-1	97	8.34	1.6000	140	12.44	1.5520
4e-1	225	20.07	1.6000	207	18.75	1.5520
6e-1	349	30.82	1.6000	297	26.92	1.5520
8e-1	493	42.85	1.6000	445	40.04	1.5520
1	659	56.75	1.6000	548	47.31	1.5520

Table 6: Number of iterations and CPU time for NSOR_ada with different values of $\beta_1 \equiv \beta_2$; $\varepsilon = 1e-5$ and $\omega^0 = 1.6$, largest 1000x500 images from Table 3.

		Image 1		**Image 2**	
β_1	$\omega_{Opt}^{\mathbf{A}}$	Iters.	CPU	Iters.	CPU
5e-4	1.0	1	1.41	1	1.47
7e-4	1.0	2	1.52	2	1.51
9e-4	1.0	7	1.98	6	1.89
2e-3	1.05	9	2.16	9	2.17
4e-3	1.09	14	2.63	16	2.81
6e-3	1.22	13	2.58	13	2.54
8e-3	1.24	13	2.60	15	2.76
1e-2	1.26	15	2.74	15	2.76
3e-2	1.51	28	4.40	27	4.31
5e-2	1.62	38	5.95	35	5.51
7e-2	1.63	47	7.17	38	6.03
9e-2	1.66	43	6.75	44	6.88
2e-1	1.76	67	9.81	67	9.88
4e-1	1.80	104	14.48	86	12.19
6e-1	1.84	126	17.16	115	15.93
8e-1	1.87	138	18.50	134	17.99
1	1.87	209	27.12	140	18.73

Table 7: ω_{Opt} (seeked by hand), number of iterations, and CPU time for NSOR_var with different values of $\beta_1 \equiv \beta_2$ for the largest 1000x500 images from Table 3; $\varepsilon = 1e-5$.

B Figures

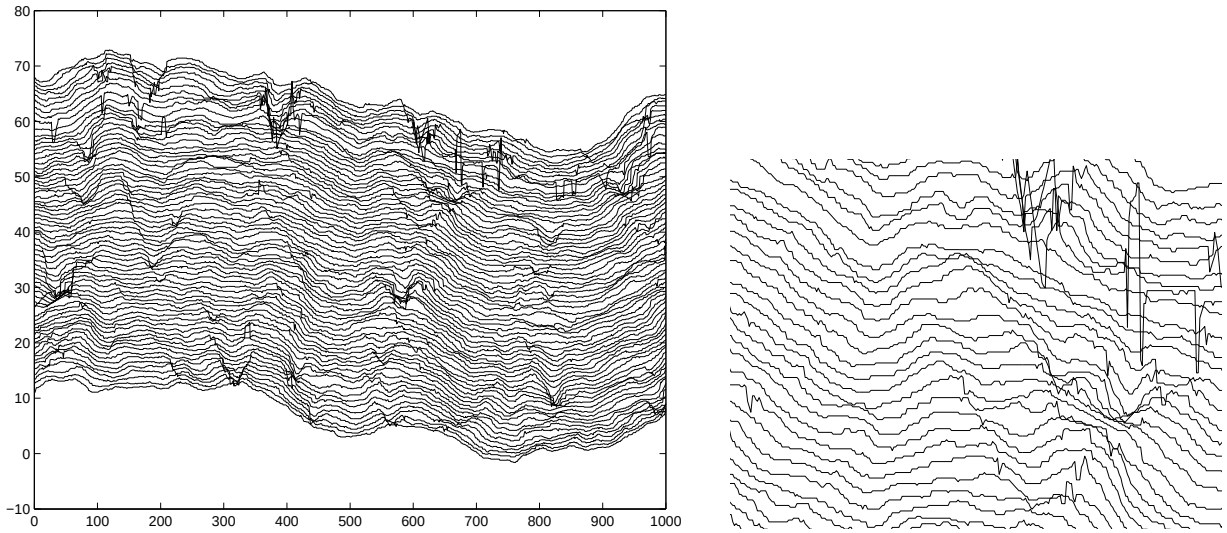

Figure 4: Original validation image (left) and a local zoom (right).

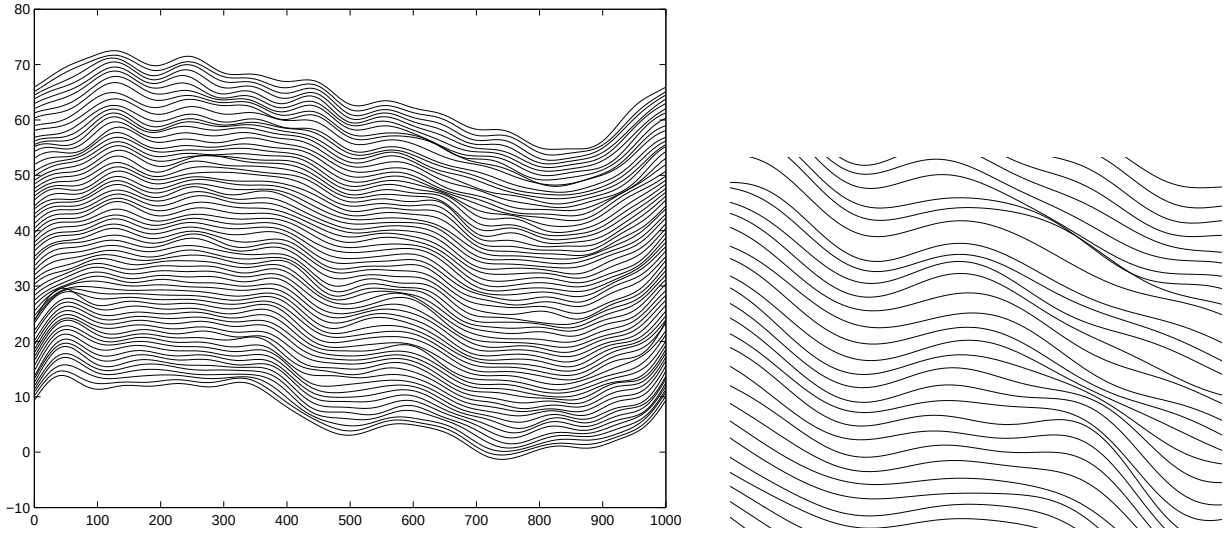

Figure 5: Denoised front profile using Fourier filter: restored validation image (left), local zoom of the result (right).

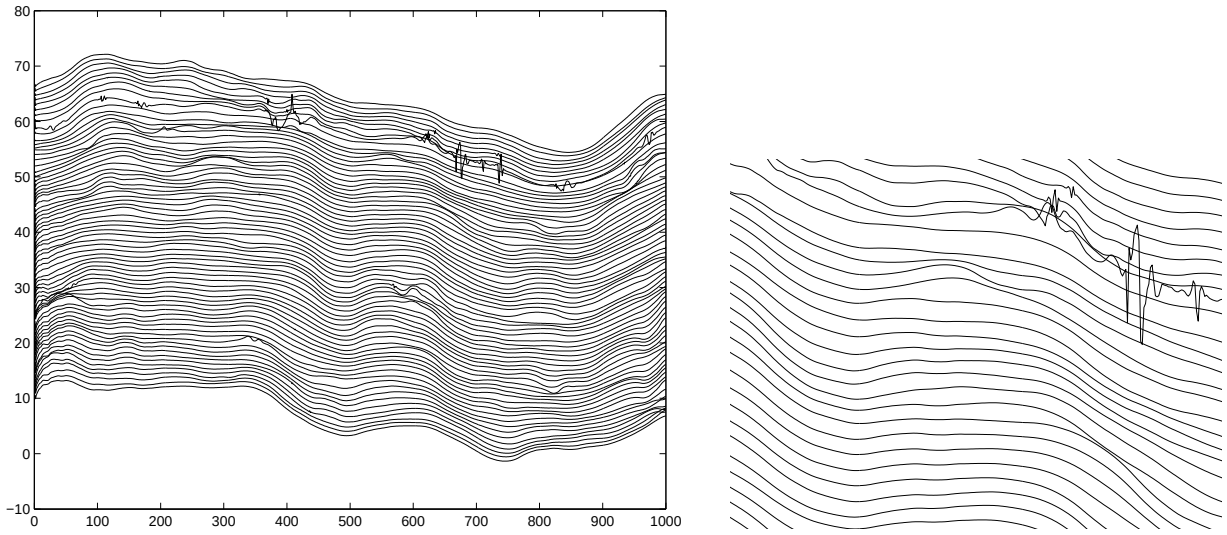

Figure 6: Denoised front profile using Wavelet filter: restored validation image (left), local zoom of the result (right).

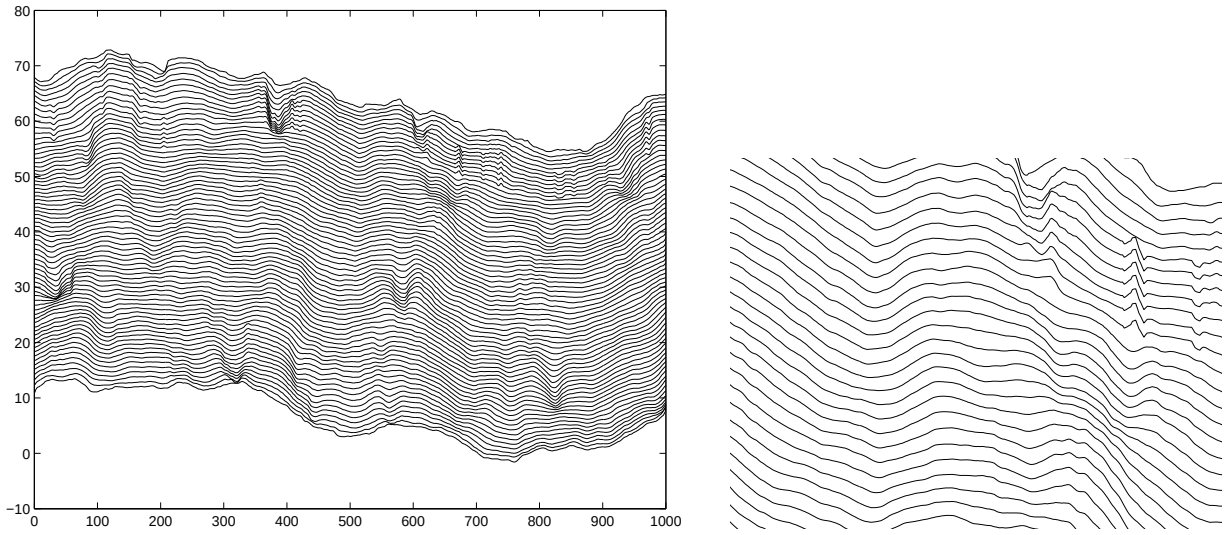

Figure 7: Denoised front profile using mean filter: restored image (left), local zoom of the result (right).

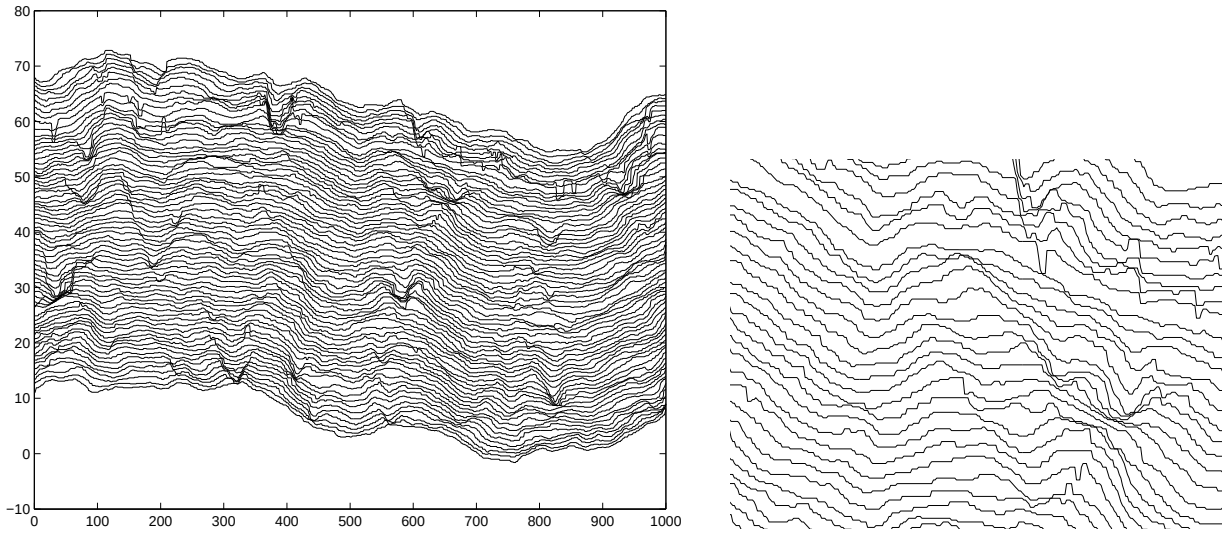

Figure 8: Denoised front profile using median filter: restored image (left), local zoom of the result (right).

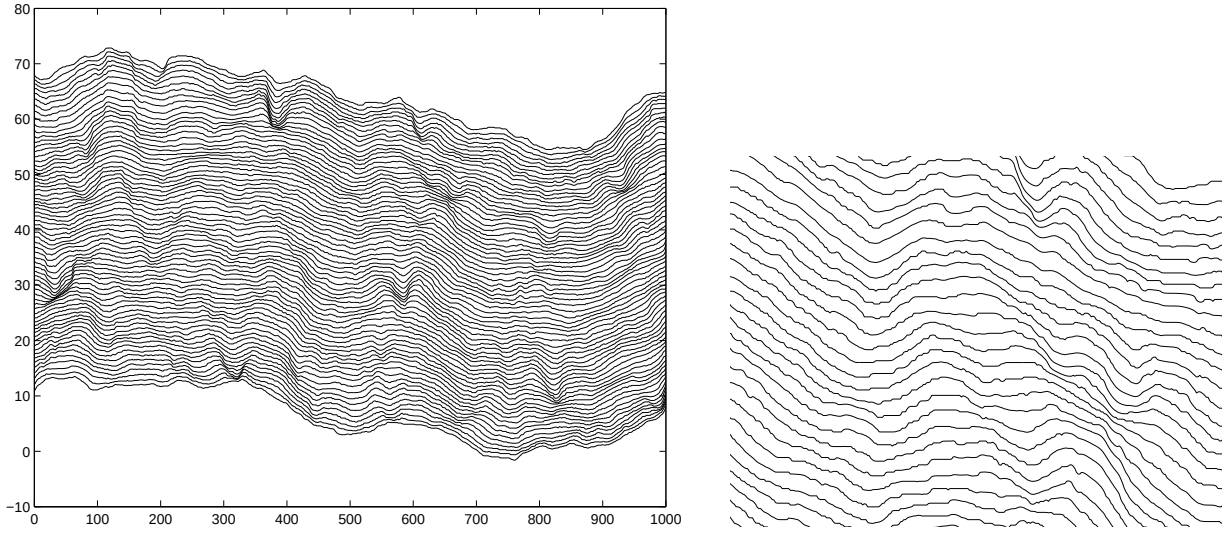

Figure 9: Denoised front profile using L_1-filter: restored image (left), local zoom of the result (right).